Research Signpost
37/661 (2), Fort P.O., Trivandrum-695 023, Kerala, India

Protein Structures: Kaleidoscope of Structural Properties and Functions, 2003: 405-439 ISBN: 81-7736-177-5
Editor: Vladimir N. Uversky

18 GFP-like fluorescent proteins and chromoproteins of the class *Anthozoa*

Vladislav V. Verkhusha [1], Mikhail V. Matz [2], Takeshi Sakurai [3] and Konstantin A. Lukyanov[4]
[1]Department of Pharmacology, University of Colorado Health Sciences Center, Denver CO 80262, U.S.A.; [2]Whitney Laboratory, University of Florida, St. Augustine, FL 32080 U.S.A.; [3]Yanagisawa Orphan Receptor Project, JST, National Museum of Emerging Science and Innovation, Tokyo 135-0064, Japan; [4]Institute of Bioorganic Chemistry of Russian Academy of Sciences, Moscow 117997, Russia

Abstract

Intensive searches for novel GFP-like fluorescent proteins and non-fluorescent chromoproteins from class Anthozoa have identified about 100 distinct genes that, together with jellyfish Aequorea GFP mutants, cover the emission range from 442 to 645 nm. Despite spectral and chromophore diversity, Anthozoa members of the GFP-like protein family possess significantly similar structural, biochemical and photophysical features. These features are reviewed here, based on studies of DsRed1, DsRed2, M355NA and HcRed1 red fluorescent proteins. In addition to emphasizing their many advantages we also point out the limitations of their applications

Correspondence/Reprint request: Dr. Vladislav V. Verkhusha, Department of Pharmacology, University of Colorado Health Sciences Center, Denver, CO 80262, U.S.A. E-mail: vlad.verkhusha@uchsc.edu

in cell biology research and biotechnology due to their oligomeric nature and tendency to nonspecifically aggregate. Although multistep mutations may create monomeric proteins, as in the case of DsRed1, other approaches exist that enable the use of Anthozoa proteins as multicolor non-cytotoxic reporters and protein fusion tags. Analysis of the formation mechanisms and light-induced photoconversions of Anthozoa chromophores has enabled us to discuss fluorescent timer and photoactivated labeling applications.

1. Introduction

Fluorescent bioimaging of single molecules, intact organelles, live cells and whole organisms has become an invaluable approach in the fields of biochemistry, biotechnology, cell and developmental biology [1]. Cloning of green fluorescent protein (GFP) from the jellyfish *Aequorea victoria* (class *Hydrozoa*) [2], and subsequent creation of wavelength-shifted and enhanced mutants such as EBFP, ECFP, EGFP [3,4,5] and EYFP [6], have made enormous impacts on biological research. Further crucial breakthroughs have come with recent cloning of novel GFP-like green, yellow and red fluorescent proteins (FPs) [7-10] and non-fluorescent chromoproteins (CPs) [10-12] from class *Anthozoa*. GFP-like proteins are a fast growing family of homologous 25-30 kDa polypeptides that currently consists of about 100 cloned genes from *Anthozoa* and *Hydrozoa* species.

In comparison to other natural pigments [13], GFP-like proteins stand out because they form internal chromophores without requiring accessory cofactors, external enzymatic catalysis or substrates other than molecular oxygen [3]. This gives GFP-like proteins many advantages over low-molecular weight probes and other FPs and CPs. These advantages include chromophore formation being possible in live organisms, tissues or cells while maintaining their integrity [14], as well as molecular, organelle or tissue targeting and specificity [15]. Due to β-barrel structures, GFP-like proteins are also extremely useful in studies of folding pathways and thermodynamics of intermediates of predominantly β-folded proteins [16]. Finally, increasingly they are used as quantitative genetically encoded reporters for second messengers, intracellular chemical environments, protein-protein interactions, and protein and cell tracking [17].

Whereas more than six thousands publications describe studies and applications of *Aequorea* GFP and its mutants (PubMed), only about 1% describe *Anthozoa* FPs, with most of those reporting on the red fluorescent protein, DsRed1 (drFP583) from the indo-pacific corallimorph *Discosoma sp*. [7]. Therefore, while referring the reader to the recent review on Aequorea GFP [18], here we will concentrate on spectral and structural properties, biochemical and evolutionary characterization, biotechnological and cell biological applications of *Anthozoa* members of the GFP-like protein family in particular.

2. Homology and spectra

Several decades ago GFPs were identified in *Aequorea* jellyfish [19] and *Renilla reniformis* sea pansy [20] as components of their bioluminescent system. These GFPs act as secondary emitters that transform blue light emitted by photoprotein or luciferase, into green light. The association of GFPs with bioluminescence was probably the main

reason researchers did not search for GFP-like proteins in non-bioluminescent corals for some time. It is now clear that the vivid fluorescent and non-fluorescent coloration of coral polyps is mainly due to numerous GFP homologues [7-12,21,22].

Although amino acid homology between *Anthozoa* FPs and *Aequorea* GFP is rather low (about 25-30%), all key secondary structure elements are clearly detectable upon alignment of their sequences (Fig. 1). Each has 11 β-strands and turn motifs between them, thus the characteristic GFP β-barrel fold appears highly conserved. This observation is supported by comparing 3D structures of GFP and DsRed1 (section 4). The main special feature of *Aequorea* GFP is an ability to form a chromophore inside the protein globule by modification of amino acids at positions 65-67 (Ser-Tyr-Gly) [6,23,24,25] (section 3). In *Anthozoa* FPs, the chromophore-forming Tyr66 and Gly67 residues are invariant (we will number *Anthozoa* FP amino acids in accordance with *Aequorea* GFP). Arg96, which probably participates in cyclization, is present in all known FPs. Strong conservation of Glu222 indicates it is also important in chromophore formation [26].

The interesting feature of non-bioluminescent coral-derived GFP-like proteins is their color variety. *Anthozoa* FPs can be divided into three main fluorescent groups with respect to the appearance of the purified protein to the human eye: green (~485-520 nm, GFP), yellow (~540 nm, YFP) and orange-red (>570 nm, RFP) emitters [10]. In addition, several *Anthozoa* FPs with dual-color fluorescence (green and red) have been identified [10], as well as a group of non-fluorescent purple-blue GFP-like chromoproteins [9,11,12,21]. Although CPs effectively absorb light, they emit virtually none. Representative spectra for these color groups are shown in Fig. 2 (left row). Understanding the relationship between protein structure and spectral properties is of great scientific and practical interest. However, in spite of the abundance of sequences available, at present it is difficult to determine which amino acid positions are responsible for particular types of spectra.

Site-directed and random mutagenesis has been used to reveal important residues in GFP-like proteins. The first color transitions were obtained for non-fluorescent asulCP from the sea anemone *Anemonia sulcata* [11]. It was demonstrated that asulCP with a single amino acid substitution, A148S, became an RFP. Dual-color (green and red) fluorescent mutants of asulCP have been generated [11], in addition to a number of DsRed1 dual-color and green mutants having been characterized [27-31]. Gurskaya and co-workers demonstrated interconversion between *Anthozoa* GFPs and YFPs, and the appearance of an additional red peak in *Anthozoa* GFP [32]. Fluorescent mutants of CPs were generated [12], and vice-versa, a true non-fluorescent chromoprotein, DsRed-NF was made from DsRed1 [33]. The main color transitions achieved by mutagenesis, and the corresponding crucial amino acid positions, are presented in Fig. 2 (right column) and Fig. 3, respectively. 3D structures for *Aequorea* GFP and DsRed1 show that the majority of positions responsible for color change are located near the chromophore.

Particular attention has been focused on creation of red-shifted FP mutants, which are in high demand for various practical applications. Natural *Anthozoa* RFPs identified to date have fluorescence maxima no more than 595 nm [8,10]. A red-shifted mutant emitting at 616 nm, ds/drFP616, was created using a shuffling DsRed1 and dis2RFP, followed by random mutagenesis [8]. The further red shift were achieved in fluorescent

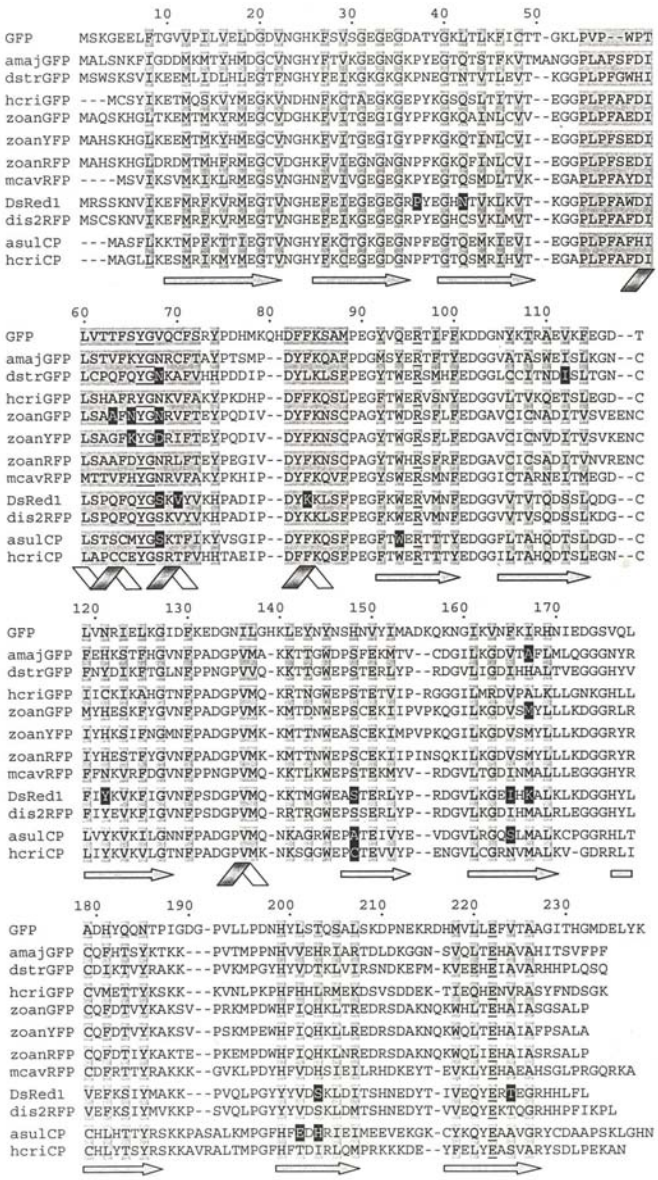

Figure 1. Polypeptide sequence alignment of the GFP-like protein family. Representatives from different color groups are shown: amajGFP and dstrGFP for the cyan subgroup of GFPs, hcriGFP and zoanGFP for GFPs, zoanYFP for YFPs, DsRed1 and dis2RFP for RFPs, and asulCP and hcriCP for CPs. ZoanRFP and mcavRFP represent subgroups of dual-color RFPs. Numbering is based on *Aequorea* GFP. Introduced gaps are represented by dashes. Conserved Tyr66, Gly67, Arg96 and Glu222 residues are underlined. Residues whose side chains form the interior of the β-barrel are shaded. Amino acid positions crucial for color transitions are labeled in white on black. Elements of FP secondary structure are outlined below the sequence.

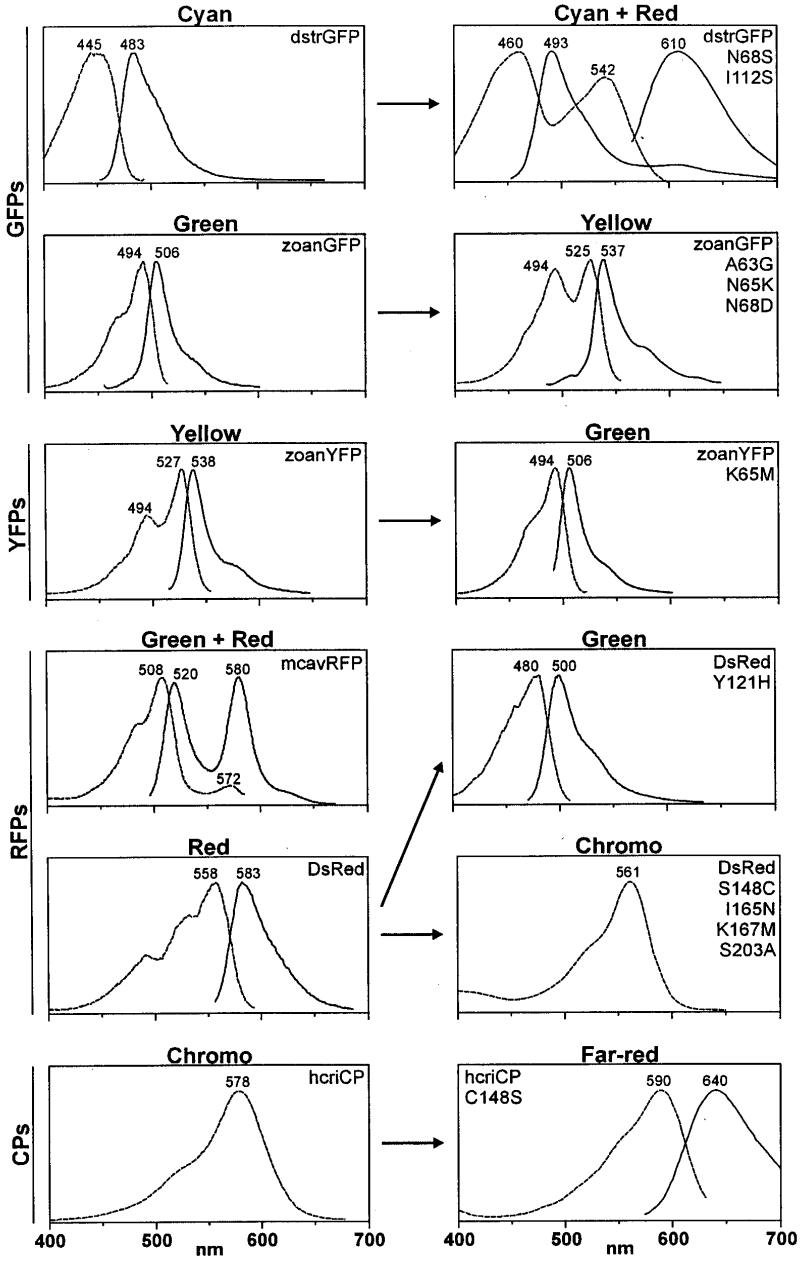

Figure 2. Spectral properties of wild-type and mutant GFP-like proteins of the main color groups: GFPs, YFPs, RFPs and CPs. Spectra for wild-type proteins are shown on the left, spectra for corresponding mutants with altered color are shown on the right. Dashed lines represent excitation spectra for FPs or absorption spectra for CPs. Solid lines correspond to the emission spectra.

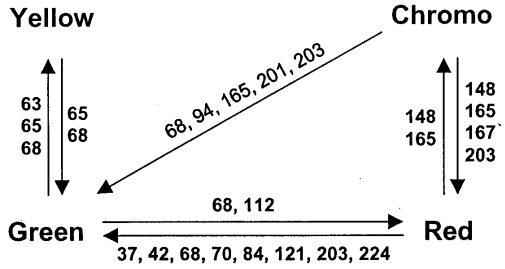

Figure 3. Main color transitions achieved by mutagenesis within the four groups of the GFP-like protein family. Numbers near arrows represent key amino acid residues substituted in mutants with changed color.

mutants of CPs. HcRed, a far-red fluorescent mutant of hcriCP from *Heteractis crispa*, possessed excitation and emission spectra peaks at 590 and 645 nm, respectively [12]. A monomeric mutant of DsRed1, mRFP1, was recently generated and has red-shifted spectra (excitation 584 nm and emission 607 nm) [34]. Of red FPs, mRFP1 is the one most likely to be as widely and safely applicable as *Aequorea* GFP variants.

3. Mechanisms of chromophore formation

Aequorea GFP chromophore formation is a self-catalyzed process consisting of cyclization of Ser65-Tyr66-Gly67 residues within the internal α-helix, followed by dehydrogenation of the Tyr66 side chain [6,23-25]. In its final form (4-(*p*-hydroxybenzylidene)-5-imidazolone), the GFP chromophore comprises two cyclic structures (Fig. 4). One cycle originates from Tyr66 itself, and the other, a 5-membered

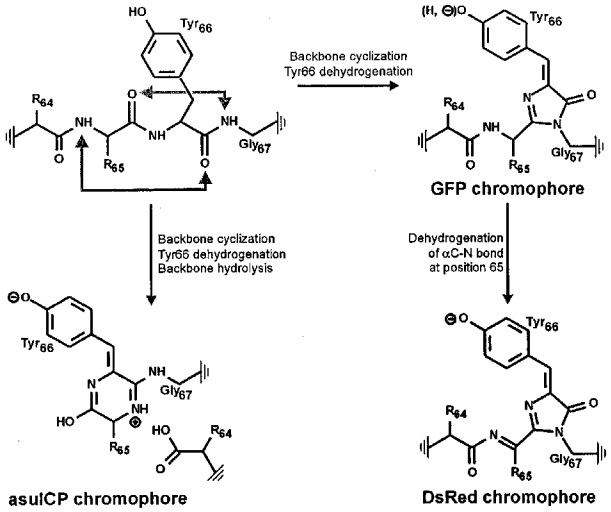

Figure 4. Scheme showing different chromophore formation in GFP-like proteins. See details in the text.

heterocycle, forms upon binding of the Gly67 nitrogen to the carbonyl carbon of Ser65. The result is a system of conjugated double bonds which are capable of absorbing violet-blue light and emitting in the green spectral region.

Anthozoa GFP-like proteins are characterized by dramatic variability in their absorption maxima. One can suggest three plausible explanations for the structural basis of these color differences. First, spectral difference could arise from distinct noncovalent interactions of the chromophore with its microenvironment. Second, GFP-like imidazolidinone structures might be extended by additional chemical reactions. Third, chromophore formation might occur via an alternative pathway yielding a distinct heterocyclic structure. Apparently, all three possibilities might be embodied among diverse *Anthozoa* FPs. Influence of the chromophore environment on spectral changes is well documented for number of *Aequorea* GFP mutants [35].

Study of the DsRed1 chromophore led to the hypothesis that RFPs contained absorbing structures chemically distinct from GFP [7]. Indeed, strong spectral red shift in DsRed1 could hardly be explained by peculiarities of amino acids around its chromophore. Soon afterwards, the DsRed1 chromophore structure was suggested [36] and shown to derive its spectral quality from an additional autocatalytic dehydrogenation of the αC-N bond of Gln65, which extends the GFP-like chromophore by two strongly electron-withdrawing double bonds (Fig. 4). The enlarged system of conjugated double bonds leads to significantly red-shifted spectra. Final confirmation of the DsRed1 chromophore structure was obtained in crystallographic studies of the protein, where a change from tetrahedral to planar geometry for the α-carbon of Glu65 was demonstrated [26,37]. Also, chemical synthesis of compounds similar to the DsRed1 chromophore showed that two additional double bonds in conjugation with a GFP-like chromophore resulted in significant red shift of absorption [38].

DsRed1 chromophores contain an acylimine, known to be an unstable species prone to nucleophilic attack [39,40]. The instability of this bond explains why absorption spectra for denatured DsRed1 and *Aequorea* GFP are almost identical [28,36]. This feature also provides an explanation for cleavage of DsRed1 into 18 kDa and 7 kDa fragments upon boiling, particularly at extreme pH [36]. Indeed, after denaturation of the protective protein shell, the initial step is likely to be hydration of the C=N bond, and harsher conditions are likely to lead to irreversible hydrolysis and cleavage of the peptide backbone at residue 65.

The currently accepted mechanism for DsRed1 chromophore formation is that a GFP-like green chromophore (absorption at 480 nm, emission at 500 nm) is formed, which undergoes oxidation and turns into a mature red chromophore (absorption at 558 nm, emission at 583 nm). This process was postulated on the basis of several observations. First, wild-type DsRed and many of its mutants contain green emitting species [27-30]. Second, in the course of protein maturation, green emission appears earlier than red, and then gradually decreases at the same rate as the red fluorescence grows [27,30]. Third, the chemical structure of the red chromophore implies extension of a GFP-like core [36].

However, our recent data suggest that this DsRed1 maturation scheme requires revision. Because of an efficient energy transfer between green and red monomers within a DsRed1 tetramer (section 5), the decrease in green fluorescence could be explained either by chemical transformation of the green chromophore into red or,

alternatively, by an increase in energy transfer to later-maturing red chromophores. Absorption, but not emission, measurements would discriminate between these possibilities because they could reflect the true amount of each spectral form. The only analysis of absorption spectra during DsRed1 maturation was performed by Wiehler and coworkers [28]. It was shown that freshly expressed DsRed1 has a minor blue absorption peak at 408 nm that completely disappears in the mature protein. This spectral form was attributed to a neutral state of a GFP-like chromophore. Moreover, an absolute increase in green absorption at 480 nm over all maturation times was demonstrated. Unfortunately, based on incorrect normalization of all spectra to the red absorption (558 nm), the authors mistakenly concluded about the relative decrease of the green peak during DsRed1 maturation.

Analysis of absorption curves generated at different stages of DsRed variant maturation shows that (i) the blue peak at 408 nm appears first, increases for some time and then falls to zero; (ii) the green peak at 480 nm appears later and increases over time; (iii) the red peak at 558 nm appears later still and also increases over time; and (iv) the decrease in the blue peak strongly correlates with an increase in the red peak (Fig. 5). These observations allow us to conclude that red chromophores originate from a blue intermediate, whereas green chromophores are a 'dead end', not an intermediate as was postulated earlier [27]. This scheme explains the previously incomprehensible observation that mature wild-type DsRed, as well as many of its mutants, contains a green form that is never converted to red.

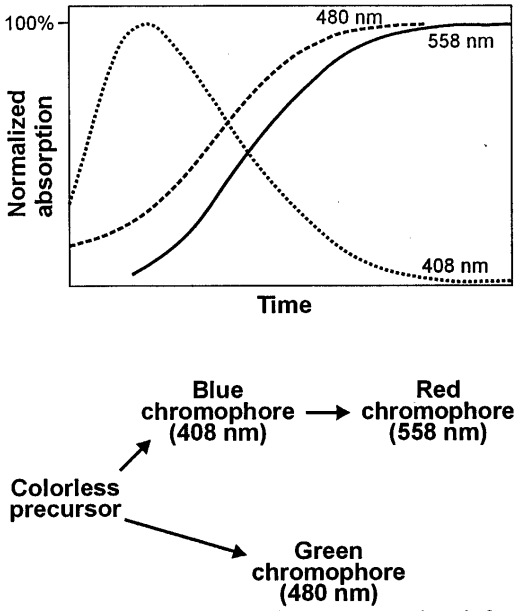

Figure 5. Time course for development of blue, green and red forms of the DsRed1 chromophore that absorb at 408, 480 and 558 nm, respectively (top). Proposed scheme for formation of these spectral forms from a colorless precursor (bottom).

Unexpected results were obtained for chromophore structures of other *Anthozoa* GFP-like proteins, such as asulCP. It was shown that in contrast to *Aequorea* GFP, another peptide bond nitrogen and carbonyl carbon are required for asulCP chromophore cyclization, a reaction that yields the six-membered heterocycle 2-(4-hydroxybenzylidene)-6-hydroxy-2,5-dihydropyrazine (Fig. 4) [42]. The amidinium group with a positive charge probably accounts for the protein's red-shifted absorption spectrum. When the asulCP chromophore cyclizes, the bond between residues 64 and 65 hydrolyzes, splitting the chromoprotein into 8 kDa and 20 kDa fragments. In contrast to DsRed1, fragmentation of asulCP is a key step in formation of a mature chromophore.

Yet another fluorescent protein, yellow zoanYFP from *Zoanthus*, appears to contain a distinct chromophore of unknown structure. Similar to asulCP, upon chromophore formation the zoanYFP polypeptide becomes gaped, but possesses distinct absorption spectra for acid and alkali denatured protein when compared to both *Aequorea* GFP and asulCP [43]. Mutagenic studies also indicate that yellow fluorescence in zoanYFP represents a novel chromophore [32].

4. Protein structure and chromophore environment

The majority of naturally occurring *Anthozoa* FPs and CPs probably form tetramers in solution, even at nanomolar concentrations, as has been shown for DsRed variants, asulCP, zoanYFP, zoanGFP, asulGFP, amajGFP and ds/drFP616, by equilibrium sedimentation [27,44,45], gel filtration [8,29], native gel electrophoresis [27,46], fluorescence correlation spectroscopy (FCS) [47] and dynamic-light scattering (V.Verkhusha, unpubl.). It was estimated from equilibrium sedimentation studies that the affinity constant between DsRed1 monomers in the tetramer is 10^{-9} M [27].

Recent DsRed1 crystal structure data [26,37] indicates the protein is a tetramer (Fig. 6A). DsRed1 monomers in the tetramer appear to be arranged in anti-parallel pairs of the molecular symmetry 2 x 2 x 2 [37]. The chromophores in the tetramer form an antenna-like rectangular array of about 2.7 x 3.4 nm, suggesting strong energetic coupling between chromophores. Crystal structures indicate angles of 21^0, 47^0 and 41^0 between different pairs in the tetramer, also suggesting energy transfer between different DsRed1 monomers.

Each DsRed1 monomer contacts the two adjacent protein molecules by two chemically distinct interfaces (Table 1). The hydrophobic interface includes a central cluster of closely packed hydrophobic residues surrounded by a set of polar side chains. The hydrophilic interface contains many salt bridges and hydrogen bonds between polar residues and buried water molecules, and also includes an unusual "clasp" formed by several C-terminal residues of each monomer. The two published DsRed1 structures differ in respect to the positioning of two C-terminal residues, Phe231 and Leu232. Yarbrough and co-workers placed Phe231 in a slot between Agr223 and Glu225 of the adjacent monomer [26]. In contrast, in the crystal structure resolved by Wall and co-authors, this slot is occupied by Leu232, while Phe231 does not participate in tetramer formation [37]. It may be that both conformations occur in nature.

Comparison of interface-forming residues in *Anthozoa* FPs (according to their sequence alignment with DsRed1) de monstrates high conservation of the tetrameric

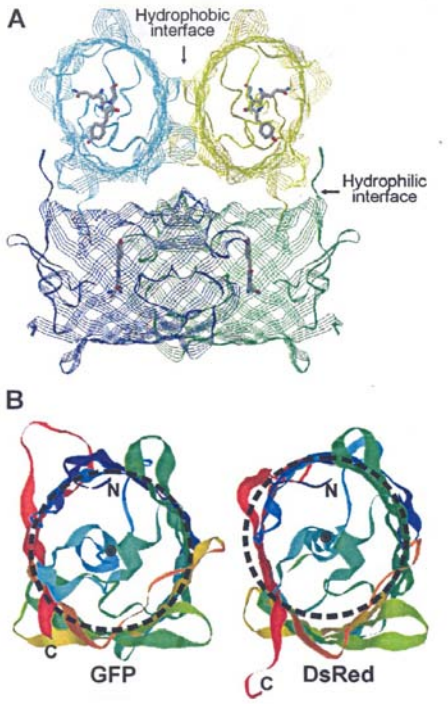

Figure 6. Overall DsRed1 structure. (A) Strand diagram of the DsRed1 tetramer. Monomers are shown in different colors. Chromophores are represented as a "sticks" model. Carbon, nitrogen and oxygen atoms are gray, blue and red, respectively. (B) Comparison of *Aequorea* GEP and DsRed1 monomers (ribbon diagram, view from the end of the β-barrels). Each chain is colored by gradient from blue (N-terminal) to red (C-terminal). A perfect circle (dashed line) is inscribed in the GFP and its center is shown. The same circle is overlaid on DsR ed1 to demonstrate deformation of its barrel. The structures were generated by Rasmol software.

structure among GFP-like proteins (Table 1). At the same time, some specific features can be found in almost every protein. For instance, rfloRFP probably does not contain salt bridges around the hydrophobic interface since it carries Val19, Pro26 and His124 rather than the interacting Glu19, Lys124 and Glu26 in DsRed1. Also, rfloRFP lacks Arg157 that would interact with Glu101 in a hydrophilic interface. In contrast, mcavRFP possibly contains a salt bridge within the hydrophobic interface between Arg109 and Asp126. Interestingly, all three closely homologous *Zoanthus* FPs (zoanGFP, zoanYFP and zoan2RFP) possess clearly distinct interfaces, with differences at positions 109, 124, 126, 128 and 157. It is likely each protein tries to form homo- rather than heterotetramers. In addition, fluorescence microscopy of live corals demonstrates that FPs of different colors are usually expressed in different cells of the organism. Therefore, we believe it unlikely there are mixed FP tetramers in nature [37].

At physiological concentrations, wild-type FPs of the bioluminescent representatives of GFP-like family, including *Aequorea* and *Renilla* GFPs, are capable of forming heterotetramers with their respective photoproteins (GFP_2 x $photoprotein_2$) [48]. These

Table 1. DsRed1 teramer interface-forming residues and their conservation and variability in other GFP-like proteins.

Amino acid positions and their interactions		DsRed1	mRFP1	dstr GFP	amaj GFP	zoan GFP	zoan YFP	zoan RFP	rflo RFP	mcav RFP	asul CP	hcri CP
Hydrophobic interface	97	V	V	S	T	S	S	S	T	S	T	T
	105	V	V	L	V	V	V	V	V	I	F	I
	107	T	T	C	T	I	I	I	T	T	T	T
	109	T	T	T	S	N	N	S	T	R	H	H
	126	I	R	T	H	Y	N	Y	M	D	L	L
	128	V	T	L	V	V	M	V	A	V	N	T
	184	I	T	V	S	V	V	I	I	T	T	S
	19	E	E	E	D	E	E	E	V	E	E	E
	124	K	K	K	T	K	I	T	H	R	K	K
	26	E	E	Y	Y	K	K	K	P	N	Y	Y
Hydrophilic interface	101	E	E	E	E	E	E	E	E	E	E	E
	157	R	E	R	C	K	K	S	C	R	V	E
	166	H	K	H	T	S	S	S	A	N	L	V
	180	E	E	D	Q	Q	Q	Q	D	D	H	H
	153	Y	Y	Y	T	I	M	I	F	Y	Y	Y
	176	H	H	H	N	R	R	R	H	H	H	R
	178	L	D	V	R	R	R	R	R	R	T	I
	151	R	R	R	K	K	K	K	I	K	I	V
	168	A	R	A	F	Y	Y	Y	S	A	A	A
	146	E	E	E	D	E	E	E	E	E	E	E
	198	Y	A	Y	N	W	W	W	Y	Y	F	F
	200	Y	K	Y	V	F	F	F	F	F	F	F
	147	A	A	P	P	P	A	P	P	P	P	P
	149	T	T	T	F	C	C	C	T	T	T	T
	229	H	S	H	T	S	S	S	S	G	C	S
	230	L	T	P	S	A	A	A	P	L	D	D
	231	F	G	F	V	L	L	L	L	P	A	L
	232	L	A	Q	F	P	A	P	Q	R	A	P
	223	R	R	I	H	H	H	H	G	H	A	A
	225	E	E	V	V	I	I	I	V	E	V	V
	204	K	K	K	R	K	K	K	C	S	R	R

observations, together with structural studies, suggest the β-barrels of GFP-like proteins have two distinct interfaces that interact with other subunits. One of these interfaces is usually involved in formation of homodimers, but the function of the other has diverged during evolution; in bioluminescent species it binds aequorin or luciferase, whereas in non-bioluminescent organisms it binds the second dimer of the GFP-like protein. Additionally, distinct interfaces might evolve to maximize thermotolerance or

photostability of GFP-like proteins under intensive sunlight. This correlates with the observed optimal FP folding efficiencies (32-38^{0}C for DsRed1 [29,49]), and presence of a 330-340 nm absorption peak in red chromophores of coral-derived RFPs, which accepts emission from UV-absorbing tryptophanes and transfers it to red chromophores. In contrast, *Renilla* and *Aequorea* GFPs fold better at lower temperatures and do not have far-violet absorption [50].

Knowledge of DsRed1 tetramer structure provided a basis for creating mutants of interface-forming residues to generate non-oligomerizing FPs. Mutagenic studies demonstrated tetramerization was very important for FP maturation. Single amino acid substitutions of interface-forming residues in DsRed1 resulted in a sharp drop in fluorescence intensity and maturation speed [34]. However, different *Anthozoa* proteins appeared to have different sensitivity to tetramer disruption. A fluorescent mutant of hcriCP was easily converted to a dimer by a single L126H substitution within the hydrophobic interface, without a significant decrease in brightness [12]. For DsRed1, mutation at the same position (I126R) also resulted in a dimeric protein, but in this case the dimer was almost non-fluorescent [34]. Subsequent mutagenesis rescued fluorescence in dimeric DsRed. A truly monomeric mutant, mRFP1, has been created which contains three amino acid substitutions within the hydrophobic, and ten within the hydrophilic, interfaces (Table 1).

Overall folding of the DsRed1 monomer is very similar to that of *Aequorea* GFP, consisting of an 11-stranded β-barrel with a central chromophore-bearing helix and α-helical caps on the barrel ends. The most interesting peculiarity of DsRed1 is noticeable deformation of its β-barrel (Fig. 6B). In contrast to *Aequorea* GFP, which is almost perfectly circular when viewed from the end of the barrel, the DsRed1 monomer is an oval. This deformation has direct consequences on the chromophore microenvironment and is probably important for protein maturation. It is tempting to speculate that barrel flattening is forced by interactions of the monomers in the tetramer. This could explain the loss of fluorescence in mutants with affected tetramer interfaces.

The DsRed1 chromophore was found to be rather similar to GFP chromophore, and consists of the same planar *p*-hydroxybenzylidene imidazolinone core originating from cyclization of the backbone between Gln65 and Gly67, and following dehydrogenation of the Tyr66 Cα-Cβ bond (Fig. 7A). However, the Glu65 Cα was observed to be planar and sp^2 hybridized, due to formation of a double C=N bond at position 65. These crystallographic studies are consistent with determination of DsRed1 chromophore structure by organic chemistry approaches [36]. The chromophore environment in DsRed1 consists of an extremely polar cavity, which includes a complex network of hydrogen bonds and salt bridges. Selected neighboring residues of the chromophore are shown in Fig 7. The phenolate oxygen of the chromophore's Tyr66 forms a hydrogen bond with Ser148 (Fig. 7B). Ser148 is invariant in all *Anthozoa* FPs, but absent in all CPs. Contact between Tyr66 and Ser148 is apparently very important for generation of fluorescence because it appears to stabilize the chromophore. This is consistent with mutagenesis studies that revealed Ser148 as the key residue in interconversions between FPs and CPs [11,12,33]. An interesting feature of DsRed1 is direct contact between the Tyr66 phenolate oxygen and positively charged Lys167 (Fig. 7B). None of the known FPs, including closely homologous red dis2RFP, contains Lys at this position. Random mutagenesis of DsRed1 shows that Lys167 can be substituted by Gln or Met [34].

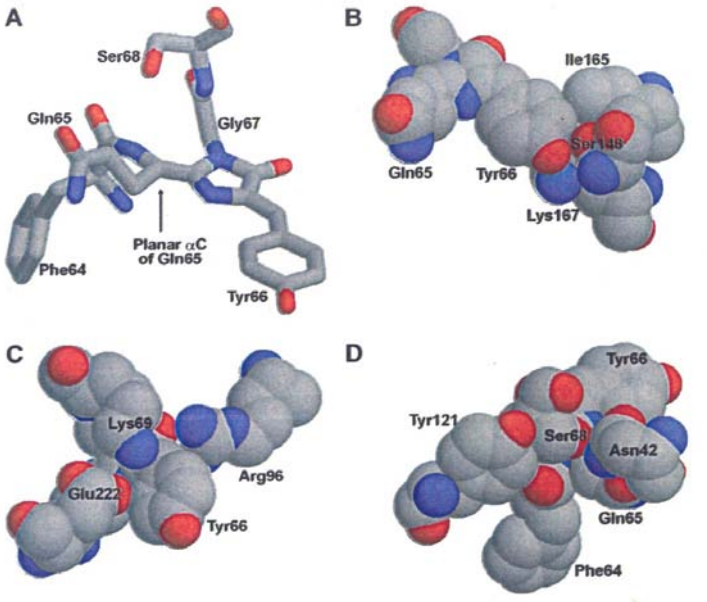

Figure 7. DsRed1 chromophore and its environment. (A) Stick diagram of residues 64-68. (B-D) Spacefill representation of the chromophore and selected neighbors. Carbon, nitrogen and oxygen atoms are gray, blue and red, respectively. The diagrams were created by Rasmol software.

Therefore this ionic contact appears to have no general significance for generation of red fluorescence.

In spite of their close proximity in DsRed1, Ser203 and Tyr66 do not form an H-bond as do Thr203 and Tyr66 in *Aequorea* GFP [6,25]. However, mutations at position 203 lead to significant spectral changes in DsRed1. S203A substitution results in faster protein maturation [31], S203T significantly increases green fluorescence in immature protein [30], while S203Y partially suppresses green emission and increases folding efficiency [49].

Position 165 also deserves special attention. In DsRed1, Ile165 is located in the plane of the chromophore and in direct contact with the Tyr66 phenolic ring (Fig. 7B), similar to the positioning of Phe165 in GFP [6,25]. Such an arrangement should prevent *cis-trans* isomerization of the chromophore around the Tyr66 methylene bridge. This isomerization is believed to be the main cause of non-radiating relaxation of the excited state of the chromophore [51,52]. Position 165 in all FPs is occupied by bulky aliphatic residues (Phe, Ile, Val, see Fig. 1). In contrast, CPs carry small hydrophilic Asn or Ser165. Mutagenesis has confirmed the importance of this distinction. For example, S165V substitution in asulCP resulted in formation of red fluorescence, while I165N mutation was found to be essential for transformation of DsRed1 into a non-fluorescent CP [33].

The middle region of the DsRed1 chromophore is in proximity with Arg96, Lys69 and Glu222 (Fig. 7C). Arg96 is invariant for all GFP-like proteins and is found in the same position in *Aequorea* GFP, making close contact with the imidazolinone oxygen.

Arg96 probably participates in catalysis of backbone cyclization. Evolutionarily conserved Glu222 in DsRed1 is closer to the chromophore than in GFP, and the importance of this residue in formation of the red chromophore was proposed by others [26]. Lys69 forms a salt bridge with Glu222. Position 69 in all *Anthozoa* GFP-like proteins is occupied by either Lys or Arg, the positive charge apparently important for polypeptide organization, independent of its particular spectral properties.

Figure 7D shows the neighbors of the most interesting part of the DsRed1 chromophore, which has the additional C=N bond at position 65. Ser68 apparently plays a role in formation of this double bond. Indeed, its Oγ atom is placed over the Gln65 Cα-N bond in a position appropriate for proton abstraction [26] (Fig. 7A,D). Other data also clearly indicate the significance of position 68 for color determination. Sequence comparison of GFP-like proteins shows that Ser68 is characteristic of many red-shifted proteins, but not of GFPs (Fig. 1). It was demonstrated by mutagenesis that insertion of Ser68 (together with Ser112) into dstrGFP results in an additional red fluorescence peak [32]. Also, Asp68 that is unique for zoanYFP, was found to be important for yellow fluorescence [32]. An interesting exception to this rule is a group of recently found natural "fluorescent timers", such as zoan2RFP, mcavRFP and rfloRFP, which change color from green to red (or to the mix of green and red) during maturation [10] (section 9). In spite of the apparent presence of a red-shifted chromophore within these proteins, they carry Asn68 that is characteristic for most GFPs (Fig. 1). These RFPs may possess a novel variant of the red chromophore, with another residue(s) participating in its formation.

Asn42 contacts Ser68, Gln66 and Glu222 and is important for their proper positioning. This probably explains the significant increases in green fluorescence associated with substitutions of Asn42 [28,53]. Finally, crystal structure provides a rationale for the influence of position 121 on DsRed1 maturation. Single Y121H substitution results in an almost completely green mutant ([29], M.Matz and K.Lukyanov, unpubl.) (Fig. 2). This substitution probably leads to a change in Ser68 orientation that is disastrous for the catalysis of Gln66 dehydrogenation.

5. Photophysical properties

To study intramolecular dynamics of *Anthozoa* proteins and excitation states of their chromophores in ensemble or single-molecular modes, several single and two-photon approaches of steady-state and time-resolved spectroscopy have been used. The basic photophysical parameters of fluorescence proteins, such as saturation intensity (I_s, the intensity of excitation light resulting in maximal chromophore emission yield), photobleaching time limit ($\tau_{bl\ inf}$, the time it takes the chromophore to undergo photobleaching at infinite excitation intensity) and maximal photon emission rate of the chromophore (k_{inf}), have been compared between DsRed1 and *Aequorea* GFP variants [54]. It was found that in both bulk solution and immobilizing gels, single-molecules of DsRed1 have the higher I_s (45-50 kW/cm^2) and k_{inf} (1.2-1.8x10^4 photones/ms) but lower $\tau_{bl\ inf}$ (0.3-0.4 ms), indicating that DsRed1 red chromophores are brighter, but more susceptible to photobleaching.

Application of time-correlated single-photon counting and frequency-domain fluorescence life-time microscopy (FLIM) to bulk solutions of zoanYFP, DsRed1 and some DsRed1 mutants has shown they have single exponential fluorescence decays with

similar fluorescence life-times (within 3.57-3.69 ns) when excited in single-photon mode close to their absorption maxima ([47], V.Verkhusha, unpubl.). The measured life-time values are in the upper range of fluorescence life-times found for *Aequorea* GFP mutants (1.32-3.69 ns, [55]), thus allowing principal separation of these *Anthozoa* proteins from many GFP mutants in FLIM studies. DsRed1 life-time decreases with aging of bacterial cultures expressing the protein [56], probably due to non-specific aggregation of DsRed1 tetramers. By contrast, direct ensemble excitation in the absorption band of the green state of DsRed1 chromophores leads to multi-exponential decay with four components at the red emission (3.60, 0.47, 0.12 and 0.03 ns), and only three faster components at the green emission [57].

Fluorescence correlation spectroscopy (FCS) low-intensity ensemble studies of DsRed1 at 488 nm revealed a pronounced light-induced 10^3-10^4 Hz flickering process with similar characteristics observed earlier with *Aequorea* EYFP [47]. Due to this similarity the conclusion was drawn that in the presence of light DsRed1 cycles between bright and dark states with a constant partition fraction. Further single-molecule FCS analysis at excitation 543 nm (closer to absorption maximum) and higher excitation intensities, demonstrated that DsRed1 tetramers have at least three distinct fluorescent states between which light-induced cycling can be observed [58]. Moreover, two-photon FCS at 850 nm excitation showed that effective depopulation of less fluorescent states resulted in a decreased flickering fraction of the protein and increased signal-to-noise ratio. Together with large two-photon excitation cross-sections, approximately 100 GM at 990 nm [47,56], it appears DsRed mutants are likely to be the best genetically encoded tags for two-photon fluorescence imaging in live cells.

Time-resolved fluorescence anisotropy of DsRed1 with 490 nm excitation, in addition to slow rotational motion with a characteristic time of 53 ns due to the tetrameric structure, has also revealed a rapid depolarization process with a time constant of 211 ps that was attributed to intra-oligomer energy transfer between nonparallel chromophores with the initial anisotropy, implying a 24^0 depolarization angle [47]. Further picosecond time-resolved studies in 50% glycerol confirmed Forster-type fluorescence resonance energy transfer (FRET) between green and red monomers within the tetramer [59]. Ensemble fluorescence decays revealed that 25% of DsRed1 monomers with green chromophores are present in tetramers containing only this green form [57]. They are responsible for the weak green fluorescence at 500 nm. The remaining 75% of the green species are involved in FRET to the red monomers. However, dual-color single-molecule studies performed by near-field scanning optical microscopy detected only 9% of completely green DsRed1 tetramers [60]. The same experiments also showed that the relative ratios of tetramers consisting of 0, 1, 2, 3 or 4 green monomers are 13:21:36:26:4, respectively, thus resulting in a total red-to-green monomer value of 12:15.

The rate constants for energy hopping between identical chromophores were calculated from DsRed1 crystallographic data [61], and predicted multilevel emission characteristics for packed multichromophoric systems [62] was observed experimentally using single-molecule spectroscopy. Energy transfer between identical red chromophores occurs via coupling of transition dipoles of monomers and, partially, by excitonic exchange [63], with emission proceeding from only one chromophore in the tetramer. Because calculated rates of energy transfer between dipoles are much faster

than emission rates [61], fluorescence is essentially likely to arise from any of the four chromophores in the tetramer. This produces a four-level intensity distribution for the DsRed1 tetramer that follows a pattern of 40:26:15:7 [60].

Upon photodissociation caused by high-intensity excitation, photodynamically damaged DsRed1 chromophores are converted into a form that may still absorb efficiently, trapping the energy from the absorbed photon and partially quenching fluorescence of remaining intact monomers. Indeed, weak quenching of fluorescence on photodissociation of red chromophores in DsRed1 tetramers was detected [60]. Single-molecule experiments and crystallographic data show that a single dissociated chromophore in the tetramer quenches 27, 6 and 0.2% of the fluorescence of the nearest, intermediate and most distant monomer, respectively, with a total quenching efficiency of 33%. This effect was confirmed by ensemble studies of DsRed2 and M355NA (red fluorescent mutant of asulCP) tetramers [11,46], where three of the four fluorescent monomers were replaced by DsRed-NF [33] and asulCP/A148C non-fluorescent mutants [64], respectively. Emission intensities were reduced by about 70% in both cases, which was in good agreement with the quenching efficiency value of 66.4% estimated for three quenchers per DsRed1 tetramer.

6. Fluorescence acquisition and stability

Fluorescence development in wild-type *Anthozoa* RFPs is much slower than in *Aequorea* GFP mutants and proceeds through intermediate blue and green emissions of GFP-like chromophores (section 3). The green fluorescence component of immature DsRed1 develops as rapidly as *Aequorea* EGFP and then decreases due to FRET between green and red monomers [49]. Intensity of green emission of DsRed1 and DsRed1/S197Y was 6-10% of EGFP fluorescence, even at its peak, and about 1-3% of the mature state. Fluorescence acquisition curves of EGFP, and DsRed1 or DsRed/S197Y were qualitatively distinct over a wide range of temperatures. Logarithmic plots against time showed EGFP fluorescence increased linearly, agreeing with previously reported first-order kinetics [65]. In contrast, DsRed1 and DsRed1/S197Y showed remarkably sigmoid time dependencies that can be described by at least a three-step kinetic model [45], confirming a suggested DsRed1 chromophore formation mechanism [36]. Time required for half-maximum fluorescence development ($t_{50\%}$) decreased exponentially with temperature. The difference in $t_{50\%}$ between EGFP and DsRed1/S197Y is greater at lower temperatures and fits the equation, $t_{50\%} = 238 \times \exp((4-t^0C)/8.75)$ hours. The maximum level of DsRed1 and DsRed1/S197Y fluorescence acquisition shows a bell-shaped temperature dependency with a peak at 32-38^{0}C [49]. The final yield of fluorescence irreversibly decreased at lower and higher temperatures. No further fluorescence growth was observed when samples kept at low or high temperatures were transferred to 35°C, and fluorescence did not decrease when samples matured at 35°C were transferred to low or high temperatures. These observations indicate the presence and temperature dependence of the dead-end pathway of GFP-like chromophore maturation to a non-fluorescent state [34,49].

Several variants of DsRed1 have been created that acquire fluorescence faster than the wild-type protein. DsRed-E57 mutant matures three times faster *in vitro*, in bacteria and in *Xenopus* embryo, although it failed to increase the rate of red chromophore formation in HEK293 human cells, suggesting that fluorescence development in that

case was controlled by cell-specific rate-limiting steps [31]. A set of rapidly maturating DsRed1 mutants with half-times of 6.5-0.7 hours (2-15 times faster than wild-type protein) was generated by random and directed mutagenesis [53]. The key N42Q substitution accelerated formation of the red chromophore but also produced higher proportions of monomers with green fluorescence. Additional six rounds of mutagenesis yielded three optimized variants termed T1, T2 and T3 with rather low green emission and relative as compared to DsRed1 brightness 0.36, 0.83 and 0.38, respectively. The benefits of accelerated maturation were evident when these mutants were expressed in rapidly growing organisms. In yeast *S. cerevisiae*, mitochondria-targeted DsRed1 becomes visible only when cultures reach stationary phase, while DsRed-T4 mutants consistently gave strong fluorescence in cells from growing cultures [53]. Finally, it is worth noting that fluorescent mutants of *Anthozoa* CPs, such as M355NA [11,46] and HcRed1 [12], also acquire red fluorescence quite quickly, comparable to *Aequorea* GFP/S65T [65].

More evidence is accumulating that for GFP-like proteins, folding, rate of fluorescence maturation and final color are linked in a dynamic process. Analysis of wild-type *Anthozoa* RFPs shows that majority of them acquire fluorescence only when structurally able to form oligomers [10,27]. Comparison of DsRed mutants in the context of *Aequorea* GFP and DsRed1 crystal structures indicates that for the fast and complete maturation to red state RFPs needs sterically large free spaces around the chromophore within the primary folded β-barrel [31]. Thus, development of fluorescence is probably part of the folding process itself, and not just a final autocatalytic reaction of chromophore formation [41]. The critical chemical events for development of fluorescence and final color determination of FPs take place at rate-limiting steps along a branched pathway. Once a critical juncture is passed, the opportunity for further development is lost.

The oligomeric structure also results in higher stability and protection of internal *Anthozoa* chromophores from environmental factors compared to monomeric *Aequorea* GFP. Wild-type *Anthozoa* tetramers are non-dissociative, and are only broken down by irreversible denaturation of polypeptides. For DsRed1 and zoanYFP, it was impossible to dissociate tetramers into intact monomers by addition of low concentrations of polar or non-polar compounds, detergents, chaotropic agents, reducing agents, polyethylene glycol, ionic strength changes or changes in anion or cation concentrations [28,29,45], DsRed1 emission was quite stable despite incorporation into bis(2-ethylhexyl)sulfosuccinate-reversed micelles in organic solvents, or applying up to $3x10^3$ bars hydrostatic pressure (V.Verkhusha, unpubl.).

DsRed1 fluorescence was stable within the pH range 5.0-12.0 [27,28], which contrasts the high sensitivity of the majority of *Aeqourea* GFP mutants to mildly acidic conditions. DsRed1 emission gradually decreased below pH 5.0 and the rate and degree of this fluorescence inactivation depended on the pH value [44]. The kinetics of fluorescence inactivation fitted a two-exponential function where the initial inactivation rate was proportional to the fourth power of proton concentration. Subsequent DsRed1 alkalization resulted in partial fluorescence recovery, and the rate and degree of such recovery depended on incubation time in the acid. Recovery kinetics had a lag-time and minimally fitted a three-exponential function. The DsRed1 absorbance and circular dichroism spectra revealed fluorescence loss was accompanied by protein denaturation

[44]. Denatured DsRed1 exhibited an absorption peak at 383-387 nm, which is close to the *Aequorea* GFP maximum in similar conditions, suggesting that in the protonated state these chromophores have similar structure. A multi-step mechanism for DsRed1 tetramer behavior that includes consecutive conversion of the initial protein state, protonated by four hydrogen ions, to the denatured one through three intermediates, has been proposed, and pK_a for ionogenic groups in red monomers was estimated to be below 4.0-5.0 [27,44,45].

Thermal stability of DsRed1 fluorescence was several times higher than EGFP in the range of temperatures up to 80^0C, suggesting tetrameric packing of tightly folded β-cans preserves proteins from thermal denaturation and resultant fluorescence quenching significantly lower than in single β-barrels (Fig. 8A). The same conclusions could be drawn from unfolding studies that used detergents rather than heating, in which more than 200 h in 6.2 M guanidine hydrochloride resulted in only a 10% decrease in DsRed1 fluorescence, whereas EGFP lost half of its fluorescence within a minute (Fig. 8B). Notably, removal of detergent from denatured DsRed1 resulted in immediate recovery of green, but not red, fluorescence. The irreversible loss of red absorption and emission pointed to specific chemical modification, presumably hydration of the conjugated π-system extension, which is a characteristic of red chromophores [36]. *Anthozoa* FPs oligomeric structure probably makes them also highly resistant to the ubiquitin-based protein degradation system of intracellular proteolysis. DsRed2 co-expressed with EGFP in human HEK293 or *Drosophila* S2 cultured cells exhibited 4 times longer life-span after addition of inhibitors of transcription and translation [66]. DsRed1 fluorescence in developing *Xenopus* embryos co-injected with DsRed1 and EGFP mRNAs was also several times longer than EGFP alone [7,66]. Thus, the higher stability of *Anthozoa* RFPs favors their use in double-expression systems with *Aequorea* GFP for fluorescence sensing in extreme environmental conditions both *in vitro* and *in vivo*.

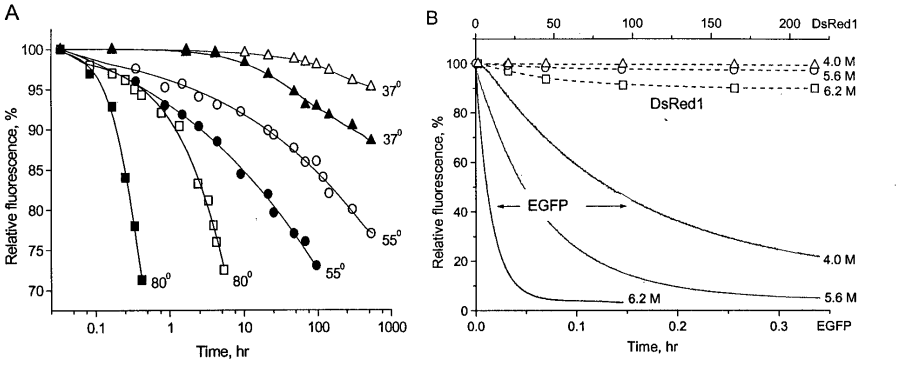

Figure 8. Stability of DsRed1 and EGFP in 50 mM Tris-HCl buffer (pH 8.0) under different temperatures and in guanidine hydrochloride. (A) Fluorescence changes of DsRed1 (open symbols) and EGFP (closed symbols) at 80 ^{0}C (squares), 55 ^{0}C (circles) and 37 ^{0}C (triangles). (B) Fluorescence changes in DsRed1 (dashed lines) and EGFP (solid lines) at the indicated concentrations of guanidine hydrochloride at 23 ^{0}C. Proteins were excited at 280 nm, and emission was detected at 510 and 580 nm for EGFP and DsRed1, respectively. Initial fluorescence intensity of each protein was valued at 100% [66].

7. Diversity and evolution

Phylogenetic diversity within the GFP-like protein family is unexpectedly high, considering the relatively low level of overall sequence divergence [10]. The likely maximum distance between coding sequences of *Anthozoa* proteins does not exceed an average of 1.5 substitutions per nucleotide (M.Matz, unpubl.). The protein family has at least four separate lineages before separation of the *Zoantharia* and *Alcyonaria* subclasses (Fig. 9). It is most surprising that, notwithstanding ancient diversity roots, emergence of new colors is very recent, with multiple independent color diversification events appearing in the most terminal parts of the phylogenetic tree. It remains to be determined whether this process of generating new colors occurs continuously within the protein family, or we are witnessing a unique event triggered by recent environmental changes.

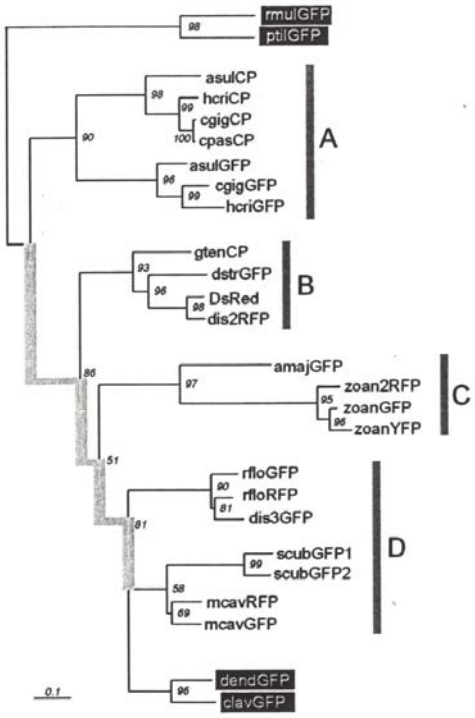

Figure 9. The maximum-likelihood phylogenetic tree of *Anthozoa* GFP-like proteins. Numbers at nodes denote the quartet-puzzling support values (10^3 puzzling attempts). Proteins from the *Alcyonaria* subclass, which were considered outgroups, are labeled in white on black. The "stem" of the tree (thick gray line), joining two rooting groups, putatively reflects the diversity of GFP-like proteins before separation of the *Alcyonaria* and *Zoantharia* subclasses. Gray bars marked A, B, C and D denote four distinct clades of GFP-like proteins found in *Zoantharia*. Scale bar: 0.1 replacements/site (Labas et al., 2002, Proc. Natl. Acad. Sci. USA, 99, 4256-4261. Copyright 2002 National Academy of Sciences, USA).

The adaptive role of *Anthozoa* coloration is still unclear. At present, photoprotection in a general sense is being discussed as the most likely functional assignment [22, 67, 68]. It was suggested that fluorescent pigments of corals serve as a screen to scatter light that reaches endosymbiotic zooxanthellae, and that this photoprotection function may be reversed to allow light collection in low-light conditions when the fluorescent layer is positioned below the zooxanthellae, rather than above [22]. Although this is the only well-formulated working hypothesis to receive some experimental support at present, there are multiple arguments against it, suggesting that it does not explain the whole story. An important observation is that the photo-modulation effects achieved by GFP-like proteins in corals must be negligible in comparison to the "built-in" photosynthesis regulation mechanisms intrinsic to zooxanthellae (M.Gorbunov, pers. comm.). Indeed, the photo-modulation hypothesis requires rigorous testing at the level of photosynthesis physiology. Another source of doubt is that in most cases the spectroscopic properties of cloned GFP-like proteins are not suitable for successful photoprotection or photoenhancement, as we discuss below.

To evaluate whether a protein is suitable for photosynthesis modulation, as suggested by Salih and coworkers [22], the excitation/emission characteristics of the protein should be related to the action spectrum of zooxanthellate photosynthesis and the spectral distribution of light in the sea (Fig. 10). For efficient protection from excessive light it is critical that the protein absorption (excitation) waveband matches the peak of photosynthesis efficiency. Ideally, emission should occur outside the waveband of maximum photosynthesis, although even emission close to excitation would provide protection due to light-scattering effects. These criteria are fully met only by proteins of the green and yellow color groups, whereas the excitation/emission range of red and purple-blue proteins shifts into the region of the photosynthesis action spectrum (Fig. 10B). As far as the light-collection function is concerned, at least with respect to stony corals (order *Scleractinia*) it seems reasonable to ask why a layer of GFP-like proteins would be a better reflector than the white aragonite skeleton underlying the living coral tissue. The only situation in which a GFP-like protein would be favorable is when the protein would transform the incoming light into wavelengths more suitable for photosynthesis. Meanwhile, the action spectrum of zooxanthellate photosynthesis corresponds well to the spectral distribution of deep-reaching light (Fig. 10A), leaving only blue light with wavelength less than 430 nm as a spectral region that could in principle be converted into the more suitable green form. Such light transformation to enhance photosynthesis was documented for the deep-water coral *Leptoseris fragilis* from the Red Sea [69]. However, in that case the fluorescent pigment was not a GFP-like protein since it was extractable by chloroform. Among GFP-like proteins, only cyan and neutral chromophore-possessing subgroups of the green color group exhibit noticeable excitation at these wavelengths, while all other colors are unsuitable (Fig. 10B).

The above considerations suggest that in regard to photomodulation, green would be sufficient, leaving unexplained the function of other colors, in particular orange-red and purple-blue, which are quite common in corals. It was suggested that red-shifted colors might serve as enhancers of green photoprotection by means of fluorescent coupling: the energy transfer from green to yellow-red pigments would result in further

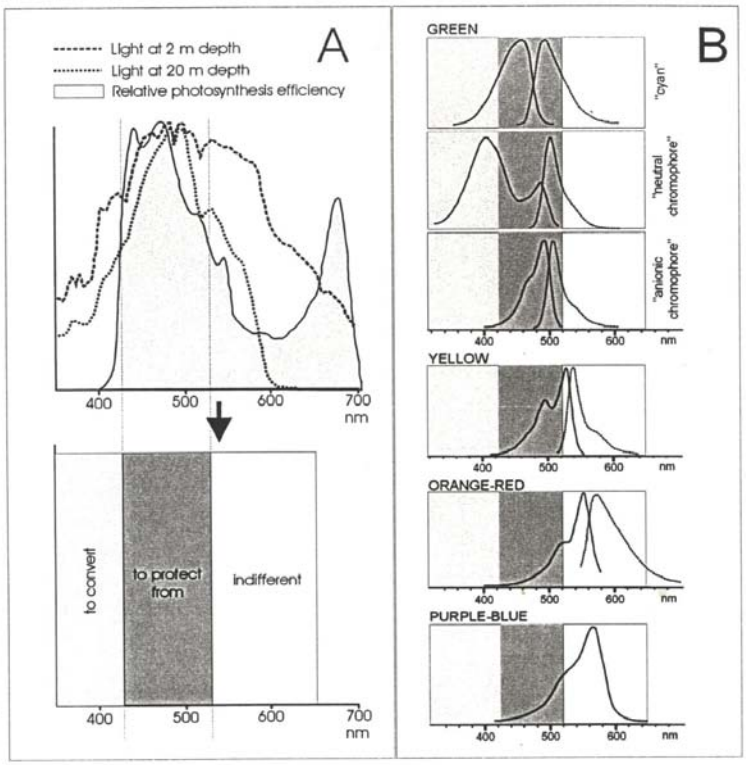

Figure 10. (A) Rough mapping of wavebands likely to be either converted into more photosynthetically suitable forms under low-light conditions, or blocked as potentially hazardous upon excessive irradiation. Top panel shows the superimposition of the spectral distribution of incoming light at depths of two and 20 m (modeled by Hydrolight software, [75]) and the action spectrum of zooxanthellate photosynthesis (shaded curve, after [76]). The bottom panel represents the conclusion. (B) Relationship of the mapped wavebands to the spectral properties of cloned GFP-like proteins of different color groups. Note that only green, and to some extent yellow, groups can be efficient blockers, while only cyan and "neutral chromophore" subgroups of the green group are suitable enhancers. Orange-red and purple-blue colors, although being quite abundant in nature, are not suitable for either function.

conversion of the incoming light into wavelengths barely affecting photosynthesis [22]. Notably, this idea requires co-localization of green and red-shifted proteins. Meanwhile, completely red-colored corals are often found, as well as green and red colors are observed in different locations within multicolored morphs [70,71,72]. It was noted that the spectral region covered by red-shifted colors roughly coincides with one of the minor absorption bands of chlorophylls *a* and *c* (so-called Q_x band). This band is poised to absorb scattered light, and therefore it is possible that red-shifted colors may in some way affect the capability of zooxantellae to utilize this particular form of irradiation [21]. However, the biological significance of this is not quite clear since it cannot have any noticeable effect on net photosynthesis efficiency.

In our view, rather than looking for a particular function for each color, the more general question to be addressed is whether color diversity is functional, or simply an accumulation of random mutations under relaxed environmental restraints [73]. Indeed, only for non-fluorescent purple-blue coloration in *Actiniaria* does the topology of the phylogenetic tree suggests that its function is different from that of green [10]: the three represented genera yielded a non-fluorescent and a green protein each, which are grouped according to color (Fig. 9, clade A). This means these colors existed as separate entities before separation of the three genera. No such color-related grouping is observed for other non-green colors. This might be viewed as an argument in favor of the "random variation" scenario; that these colors are products of accumulated random mutations under relaxed environmental restraints and have no adaptive significance of their own [73,74]. However, as we recently argued on the basis of molecular data, random changes alone are unlikely to generate and maintain the observed color diversity because of very unequal probabilities of color conversions in different directions [10]. Therefore, it seems more likely that at least some of the different colors have specific functions and are supported by natural selection. On the other hand, random mutation pressure most probably also plays a significant part in generating the diversity of colors, especially given the ease of some color conversions.

8. Passive reporters and fusion tags

Anthozoa FPs (mainly DsRed1, DsRed2, M355NA and HcRed1) have been successfully used in heterologous expression studies in a variety of cultured cells and diverse organisms such as bacteria, [56,77], yeast [78], plants [79,80], worms [30], insects [49,81,82] and vertebrates [30,83,84]. The numerous applications exploiting the red fluorescence of these proteins include their use as counter-staining and multicolor complementation for *Aequorea* GFPs [84,85], as reporters for gene activation and bacteria-based biosensors [86,87,88], as markers to study cell lineage during development [30,49], as tags for localization of proteins, organelles or virus particles in living cells [89,90,91], as population markers in symbiotic studies [92,93], and as reporters of bacterial phagocytosis and pest control [93,94]. Promoters of various strengths are suitable to drive both constitutive and inducible *Anthozoa* FPs expression, such as cytomegalovirus (pDsRed and pHcRed vectors, Clontech, CA), *c-fos* [86] and heat shock-dependent [30] promoters. *Anthozoa* FPs have also been expressed in systems that use *Sindbis* and retro viruses [85,95,96], the tetracycline transactivator (Tet-On and Tet-Off) [30] and *UAS-GAL4* constructs [49].

The advantages of *Anthozoa* RFPs as fusion tags for intracellular proteins are higher tissue translucency and lower autofluorescence in the red wavelength range, as well as perfect spectral separation from *Aequorea* GFP and its mutants, enabling multi-color cell labeling. For DsRed variants it is worthwhile noting that the C-termini of the proteins are more preferable for fusion, since the N-terminal in the tetramer is sterically remote while C-terminal residues closely surround an external β-barrel of the neighboring monomer [26,37]. Cryptic introns contained in mRNA sequences of wild-type DsRed1 and some other *Anthozoa* FPs (K.Lukyanov, unpubl.) can cause partial splicing in mammalian cells. This provides premature termination of translation resulting in less whole-length fusion protein and lower final fluorescence intensities, but can be successfully rescued

by removing putative cryptic splicing sites, as in the case of humanized version of DsRed1 (Clontech, CA).

Many *Anthozoa* GFP-like proteins, including DsRed1, also form non-specific, high molecular weight aggregates both *in vitro* and *in vivo* that cause considerable cellular toxicity [46]. This might be due to "sticky" hydrophobic patches on the molecule surface. However, since DsRed1 does not contain pronounced hydrophobic areas, aggregation may be due to electrostatic interactions. Computer-assisted calculations of DsRed1 tetramer electrostatic potentials showed its surface is mostly negatively charged except for a short N-terminal section of each monomer containing a group of positively-charged basic residues. Mutation of these residues to negative or neutral in DsRed variants and several other *Anthozoa* proteins prevented nonspecific aggregation and improved solubility [46], possibly due to breaking ionic bonds formed through the positively-charged residues.

Abnormal localization and function of tagged partners, as well as aggregation caused by the tetrameric nature of *Anthozoa* RFPs, represents a significant problem [29,96,97,98]. Furthermore, many proteins in signal transduction are activated by oligomerization, so fusion to *Anthozoa* RFPs could cause constitutive signaling. For DsRed variants this problem was finally resolved by intensive directed mutagenesis involving many rounds of evolution with several mutational steps per cycle [34]. Monomer interfaces in the DsRed1 tetramer were disrupted by insertion of positively-charged basic arginines which initially crippled the protein, but red fluorescence was rescued by random and directed mutagenesis. The final monomeric mRFP1 mutant contains 33 mutations of which 13 are internal to the β-barrel, 3 are in the short N-terminal, 13 are interfaces mutations and four are in positions where the exact effects on structure/function are unknown. Fusion of connexin43 gap junction protein to mRFP1 resulted in fully functional junctions, whereas analogous fusions to the original DsRed1 failed [97]. mRFP1 has a 1.3-times lower extinction coefficient and 3.2-times less quantum yield, but acquires red fluorescence more than 10 times faster than DsRed1, showing similar brightness to DsRed1 in living cells. Still, the drawback of mRFP1 is presence of a protein fraction with a green-absorbing chromophore that may interfere with double-labeling and FRET applications.

Several other approaches have been used to overcome aggregation of *Anthozoa* RFP fusion proteins. Covalently head-to-tail linked double copies of identical RFPs forming tandem dimers may serve as a non-oligomerizing tag. This approach was successful for HcRed1 [98] and DsRed dimeric mutants [34]. Several amino acid linkers of different lengths and compositions between the monomers were examined and the best results in terms of rate of chromophore formation and final fluorescence intensity were obtained with four and 12 amino acid linkers for HcRed1 and dimeric DsRed, respectively. Both tandem constructs displayed the same spectral characteristics as the parent proteins. Moreover, prokaryotic and eukaryotic cells possessed brighter fluorescence suggesting that protein dimerization occurs more effectively between closely linked, rather than free, monomers. Fusion of tandem HcRed1 with β-actin and fibrillarin demonstrated its superiority in *in vivo* labeling of fine cytoskeletal structures and tiny nucleoli. The resultant labeling patterns were indistinguishable from those produced by commonly used analogous EGFP-fusion constructs. Dimeric DsRed mutants linked in tandem and fused with connexin43 were also properly trafficked to the membrane and successfully

formed functional connexon channels, but were unable to assemble a large gap junction. Moreover, tandem linking significantly improved correct localization of even tetrameric *Anthozoa* RFPs such as HcRed1, DsRed2 and M355NA [98].

Simultaneous co-expression of *Anthozoa* RFP-tagged proteins with an excess of either fusion partner alone ("filling by target") or nonfluorescent mutant of respective free RFP ("filling by tag") may rescue targeting and function of fusion constructs. In the former case, connexin43 targeted with DsRed1 localized in large perinuclear aggregates, and no gap junctions in HeLa cells were observed. When either untargeted connexin43 or connexin43 fused with *Aequorea* EGFP was co-expressed, intact junctions formed containing a mixture of DsRed1-tagged and untagged, or DsRed1- and EGFP-tagged proteins, respectively [97,99]. We speculate that correct localization observed for some low-level expressed DsRed1-tagged constructs can also be explained by naturally occurring filling by free endogenous fusion partner, particularly if it is an oligomerizing protein. In the case of "filling by tag", heterotetramers consisting of RFP and the respective nonfluorescent mutants are formed, so that the four GFP-like proteins become a quasi-monomeric tag for each single fusion partner. This latter approach was applied to the M355NA-β-actin fusion construct co-expressed in L929 cells together with large amounts of nonfluorescent mutant, asulCP/A148C [64]. The actin cytoskeleton staining pattern was indistinguishable from that observed using an *Aequorea* EGFP-β-actin chimera (Fig. 11, bottom row). In both cases the larger the amount of filling used, the larger the number and length of gap junctions or actin filaments was labeled, respectively,

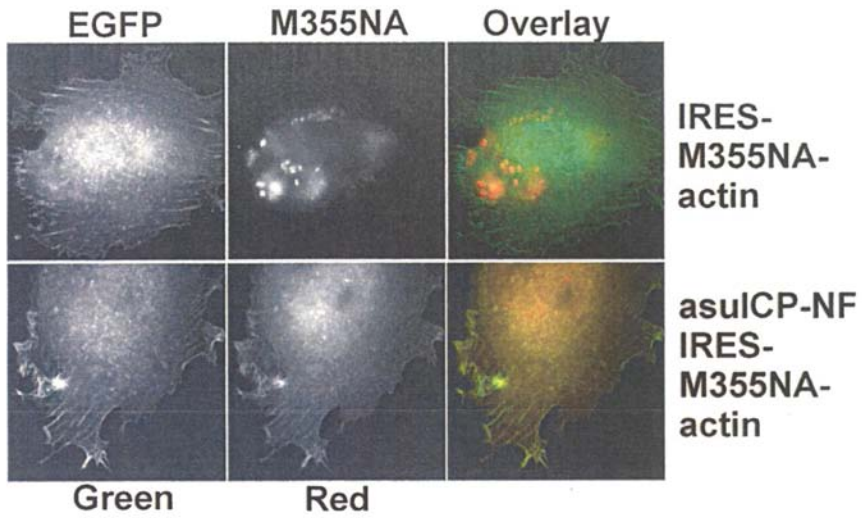

Figure 11. L929 fibroblasts cotransfected with plasmids coding EGFP-β-actin and IRES-M355NA-β-actin (upper row) or asulCP-NF-IRES-M355NA-β-actin (bottom row). EGFP-β-actin was used as a positive control to create the desired cytoskeletal staining pattern. The left column corresponds to the green fluorescent signal from EGFP, the middle column corresponds to the red signal from M355NA, and the right column represents an overlay of the left and middle images pseudocolored in green and red, respectively. Due to insertion upstream of IRES, a large excess of asulCP/A148C is produced resulting in the filling of the M355NA hetero-tetrameric tag [64].

and the lesser the aggregation of *Anthozoa* RFP-tagged proteins. “Filling by tag” can be conveniently applied to virtually any fusion partner by using a universal cloning vector containing a nonfluorescent mutant upstream of the internal ribosome entry site (IRES), while the fusion partner can be cloned downstream of the IRES in multicloning sites in-frame with the respective *Anthozoa* RFP (Fig. 11). The IRES permits translation of two open reading frames from one messenger RNA of the nonfluorescent mutant, therefore producing a large excess of the free filling for heterotetramer formation.

9. Fluorescent timer and FRET applications

The rigid β-barrel of GFP-like proteins protects their chromophores from photobleaching and environmental changes, although mutagenesis or naturally occurring peculiarities of *Anthozoa* FPs may convert them into active reporters. Wild-type *Anthozoa* RFPs (such as DsRed1) show much slower fluorescence maturation than *Aequorea* GFPs (section 6), which may be beneficial for developmental timing studies. When expressed using the same promoter at 25^0C, DsRed1 red fluorescence becomes visible approximately 18-20 hours later than *Aequorea* GFP (or EGFP) green fluorescence. If co-expression is activated shortly after generation or final differentiation of certain types of cells, fluorescence reflects the order of generation/differentiation on a whole-organism scale. Using this approach GFP and the DsRed1/S197Y mutant were expressed in the developing brain of fruit fly *Drosophila* using a *UAS-GAL4* targeting system to visualize formation order of neural fibers within large bundles [49]. Previously it was impossible to analyze the order because traditional birth date analysis involving labeling DNA-replicating cells with [^{3}H]thymidine or bromodeoxyuridine visualized only the nuclei. In contrast, GFP and DsRed1/S197Y spread into the cytoplasm of even fine cellular processes that are far from the nuclei. The results clearly showed newly extending fibers of the larval mushroom body neurons mainly run into the core of the growing bundle, rather than the periphery. Obviously, this type of double-reporter system will be useful in model genetic organisms where introducing multiple FP-reporters into one animal is possible by crossing various transformed lines.

Because maturation of DsRed1 chromophores passes through the GFP-like state (section 3) it would be attractive to use its temporary green fluorescence (later displaced by red) as a time-reflecting reporter without the need of co-expressed *Aequorea* GFPs. As already mentioned, several *Anthozoa* RFPs, such as zoan2RFP, mcavRFP and rfloRFP [10], and the DsRed-E5 mutant [30], exhibit bright green-to-red changes. Zoan2RFP and DsRed-E5 behave as absolute “fluorescent timers” in that they turn only green at first, and then mature almost completely to red. In contrast, mcavRFP and rfloRFP fail to convert completely into red even after prolonged time, resulting in a green-red two-peak emission [10]. Although the latter RFPs are not suitable for direct spatio-temporal analysis of promoter activities, the unique features of their spectra indicate that the structure of those red chromophores may be distinct from that known for DsRed1 [26,36,37].

Expression of zoan2RFP or DsRed-E5 could be used to provide precise information on activation and downregulation of target promoters. Theoretically, green fluorescent areas would indicate recent promoter activation, yellow-to-orange regions would signify continuous activation, and red fluorescent cells and tissues would denote areas in which promoter activity has ceased. To test this hypothesis, DsRed-E5 was expressed under

different promoters in several heterologous systems, and results showed that distinct green fluorescence was detected between six and nine hours after Tet-On induction in HEK293 cells, and that fluorescence was mostly red after 24 hours [30]. Also, following heat-shock promoter-regulated expression in *C. elegans*, green fluorescence was observed as early as two hours after heat shock, with red signal detected after five hours and increasing in intensity over time such that at 50 hours the red:green signal ratio was close to 9:1. Using the linearity of the red-to-green fluorescence ratio over time, DsRed-E5 was used in *Xenopus* embryos to trace *Otx-2* promoter activity involved in patterning of anterior structures [30].

Simultaneous use of two energetically distinct FPs fused to respective interacting proteins enables the creation of environment-sensing molecules. Excited-state resonance energy transfer [100] and its variants, FRET, bioluminescence (BRET) and luminescent (LRET) resonance energy transfer, in which a fluorescent or luminescent donor molecule transduces energy via a nonradiative dipole-dipole interaction to an acceptor molecule, have recently become important tools in cell biology for measurement of nanometer proximity between specific pairs of interacting proteins. Energy transfer depends on the proper spectral overlap of the donor and acceptor, the distance between them, and the relative orientation of the chromophores' transition dipoles. FRET is detectable by sensitized emission from the acceptor, decreased excited-state fluorescence life-time of the donor, or increased resistance to donor bleaching. For years such analysis was limited to proteins that could be labeled by antibodies, hormones or other ligands conjugated with suitable pairs of dyes or lanthanide elements. The creation of *Aequorea* GFP spectral mutants has enabled intrinsically fluorescent fusion constructs that localize and function as do the parent proteins to be genetically introduced into cells. Although use of *Aequorea* FRET pairs such as EBFP/EGFP and ECFP/EYFP has proved effective, there are several significant drawbacks, such as low quantum yield of the EBFP and ECFP donors, poor photostability of the EBFP donor, simultaneous excitation of the EYFP acceptor at the ECFP absorption range, and the parasitic donors' emission at the acceptor fluorescence wavelengths ("crosstalk"). Cloning of red-shifted *Anthozoa* YFP and RFPs enabled the use of two independent FRET pairs in the same cell simultaneously and resulted in increased sensitivity in analysis. While FRET approaches for intramolecular conformational changes, protein-protein interactions and intracellular signaling were thoroughly reviewed for *Aequorea* mutants [101,102], we focus on FRET features of *Anthozoa* RFPs.

The calculated Forster radii (the distances at which efficiency of FRET falls by a factor of two) for various *Aequorea* mutants and DsRed1 (assuming random relative chromophore orientation) were highest between EGFP, sapphire-GFP or EYFP, and DsRed1, with values of 4.73, 4.90 and 4.94 nm, respectively ([103], V.Verkhusha, unpubl). These values are close to the Forster radius of 4.92 nm for the best ECFP/EYFP pair, and together with the long-wavelength tail of DsRed mutants, should particularly facilitate detection of sensitized emission from these and other green and yellow donors. Indeed, when red monomers in tetrameric DsRed1 were photobleached in HeLa cells, fluorescence from green monomers increased by 2.7 to 5.6-fold in different cells, corresponding to FRET efficiencies of 68-83% [27]. These values are equal or greater than the highest efficiencies seen for *Aequorea* GFP mutants, such as 68% for ECFP and EYFP linked by a Zn^{2+}-saturated zinc finger domain [104].

Two limitations of *Anthozoa* RFPs for FRET applications include their obligate tetramerization and a broad absorption spectra causing cross-excitation of green donor and RFP acceptor. Currently, the former problem can be overcome by use of dimeric DsRed- [34] or HcRed1-tandem [98] constructs as acceptors, and the latter problem by use of the three above-indicated *Aequorea* mutants. Sapphire-GFP as well as EGFP and EYFP exhibit excitation peaks and shoulders, respectively, in the 380-460 nm range due to the presence of neutral forms of their chromophores, thus providing large Stokes shift for emission and eliminating cross-excitation with *Anthozoa* RFPs. Superiority of sapphire-GFP as the donor for DsRed1, and tolerance to its tetramerization was shown for cameleons. Cameleons represent genetically encoded FRET calcium indicators that consist of tandem fusions of FP_1-donor, calmodulin domain (CaM), CaM-binding peptide and FP_2-acceptor [105]. In HeLa cells stimulated with 10 μM histamine, different cameleon constructs with DsRed1 acceptors have shown maximal changes of about 1.10, 1.25 and 1.28 in acceptor/donor emission for ECFP, EYFP and sapphire-GFP, respectively [29]. Furthermore, in dissociated hippocampal neurons, transient calcium changes induced by depolarization caused approximately 1.32 and 1.26 ratio increases for cameleons with EYFP and sapphire-GFP donors, respectively. Suitability of EGFP as a donor for *Anthozoa* RFPs was shown using protein-protein interaction FRET assays in *Arabidopsis* plant cells [106]. PhytochromeB-EGFP- and cryptochrome2-DsRed1-tagged proteins bound each other in nuclear speckles resulting in sensitized emission from DsRed1. To ensure that the observed increase in red fluorescence was caused by FRET rather than DsRed1 re-emission of non-radiatively absorbed green fluorescence from co-localized EGFP fusion protein, the authors used a standard control involving photobleaching the acceptor that resulted in an increase of donor fluorescence.

Potential use of *Anthozoa* RFP-tandem tags as acceptors for FRET was demonstrated by changes in the emission ratio of the EYFP and HcRed1-tandem FRET pair in a protease assay [98]. A triple fusion HcRed1-tandem-EYFP protein containing the factor X_a protease cleavage site within the linker between the second HcRed1 and EYFP was produced in a bacterial system. Incubation of purified fusion construct with factor X_a led to a gradual increase in the EYFP emission peak at 528 nm and a simultaneous decrease in HcRed1 emission at 650 nm, with an isosbestic point at 625 nm (Fig.12). Protease digestion resulted in an 80% increase in yellow fluorescence and 30% decrease in red fluorescence. The ratio of donor:acceptor fluorescence changed by 2.5-fold, which was comparable with FRET levels between *Aequorea* GFP mutants [101,105,107]. Advantages of dimeric DsRed mutants linked in tandem as FRET acceptors over monomeric mRFP1, which exhibits green absorbance, are also emphasized for *Aequorea* GFP donors [34]. Tandems of Anthoza non-fluorescent mutants and CPs, such as DsRed-NF and asulCP/A148C [33], might also be useful in intracellular applications as effective fluorescence and luminescence quenchers.

Other than GFP-like proteins, donors such as organic dyes, luciferases and lanthanide elements are suitable for FRET, BRET and LRET, respectively, because they have emission that overlaps *Anthozoa* RFP absorption spectra. Among the dyes, membrane-permeant green-emitting fluorescein derivatives [108] and arsenic-based green fluorescein [109] would be useful. The latter specifically binds the unique and rare amino acid sequence CysCys-XX-CysCys added to the exogenously expressed protein,

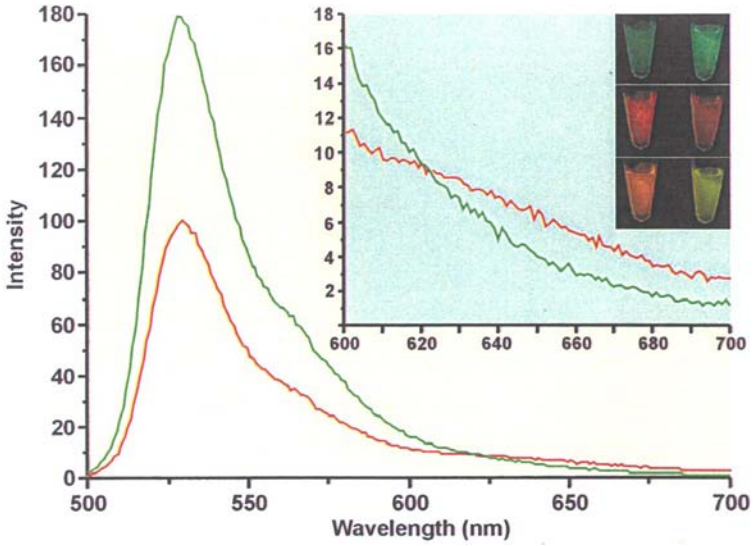

Figure 12. Emission spectra of purified triple-fusion HcRed1-HcRed1-EYFP before (red line) and after (green line) factor X_a digestion. The inset zooms in at the 600-700 nm region. The small inset in the upper right corner shows tubes with non-digested (left) and digested (right) protein samples visualized by fluorescence stereomicroscopy. The upper row depicts excitation by blue light and detection of green emission. The middle row represents excitation by blue light and detection of red emission. The bottom row represents superimposition of the upper and middle images. Increase in green signal and the simultaneous drop in red signal after digestion caused by FRET elimination are clearly distinguishable [98].

and becomes fluorescent only when bound. Yellow/orange dyes with large Stokes shift and high quantum yield, such as AttoPhos (ex. 440 nm, em. 555 nm), R-phycoerythrin (ex. 480 nm, em. 578 nm), and SYPRO Orange (ex. 480 nm, em. 568 nm) (Molecular Probes, OR), will largely reduce cross-excitations with broad absorption spectra of *Anthozoa* RFPs and provide relatively large Forster radii. A disadvantage of BRET is that it requires addition of a cofactor because of the chemical nature of bioluminescence emission, but an advantage is no cross-excitation, permitting detection of interacting proteins at much lower intracellular concentrations. Several applications of BRET using blue-emitting *Renilla* luciferase as the donor for *Aequorea* GFP mutants have already been reported [110,111], although we anticipate that insect luciferases [13], including the firefly *Luc* gene product with emission maxima in the 550-575 nm range, will result in higher efficiency of BRET with *Anthozoa* RFPs due to significant overlap of their excitation spectra. The lanthanides are uniquely luminescent elements which when chelated exhibit high quantum yields, large Stokes shifts, multi-line sharply spiked spectra in the green-red range and millisecond fluorescence life-times [112]. Terbium and europium LRET approaches are widely used in protein conformational studies [113] and in high throughput screenings [114]. Potential use of lanthanides as the donors for RFPs will make fluorescence life-time LRET detection highly suitable as it is completely insensitive to total concentration or incomplete labeling of LRET partners.

10. Fluorescent photoconverted labels

Anthozoa GFP-like proteins are remarkable in their ability to undergo photochemical transformations, which can be exploited in order to visualize diffusion or transport of FP-labeled proteins, organelles and cells. When using such labeled compounds, energetically distinct illumination of a defined spot within cells or tissues initiates the chromophore-related photochemical process. The subsequent fate of photoconverted FPs can be imaged over time, for instance, by conventional epifluorescent microscopy.

Like *Aequorea* GFPs, the majority of *Anthozoa* proteins can be irreversibly photobleached by intensive excitation at their absorption maxima for a prolonged period (usually 10-10^3 sec) in confocal or two-photon microscopy systems. The kinetics of *Anthozoa* RFP photobleaching are more complex than *Aequorea* EGFP, probably because of the complex chromophore structure or presence of several forms of the protein. DsRed and its mutants, including monomeric mRFP1, display two-exponential behavior [34,61], whereas EGFP bleaches nearly mono-exponentially. This spatially restricted photodynamic damage to chromophores allows performing fluorescence recovery after photobleaching (FRAP) and fluorescence loss in photobleaching (FLIP) studies of intracellular dynamics of FP-fused protein or FP-tagged organelles (reviewed in [115]).

In *Anthozoa* YFPs and RFPs, which have at least two different chromophore energy states (green and yellow/red [10,26,27,30,49]), photobleaching may result in color change from green to yellow/red. This means that in ensemble microscopic studies using FP tetramers containing monomers with both types of chromophore, green fluorescence is reduced while red is increased due to significant FRET between overlapping green emission and yellow/red excitation spectra. Selective photobleaching of yellow/red chromophores dequenches green emitters resulting in enhanced green fluorescence. Two-photon microscopy with excitation at 720-780 nm was used to label intracellular structures and whole DsRed-expressing cells by this “greening” technique [116]. The applied two-photon excitation was selectively absorbed by the DsRed red chromophore, which has one-photon absorption maximum at 335 nm [7], although resultant photobleaching involved a three-photon photochemical process. The green-to-red ratio increased 1.2-2.0 x10^2 times in HEK293 and CHO-K1 cells photobleached several days after transfection, and the resultant color change persisted for >30 h without affecting cell viability.

Irradiation by very intense sources in the red absorption range probably causes some *Anthozoa* RFP red chromophores to be irreversibly photoconverted to blue- and more red-shifted species. Illumination of dissolved or immobilized DsRed with a 532 nm-pulsed 120 mW laser for 14 h resulted in the 558 nm absorption peak diminishing and shifting bathochromically up to 574 nm, and a new band, about 25% of the initial 558 nm magnitude, appearing at 386 nm [57]. Importantly, the absorption band associated with the green chromophore (peak at 475 nm) was not modified with respect to position or intensity. Photoconverted DsRed excited at 390 nm had a fluorescence spectrum peaking at 500 nm, due to FRET between photoconverted blue and green chromophores, but exhibited a pronounced shoulder (50% of the maximum) at 450 nm. Moreover, when excited at 570 nm, maximum red fluorescence appeared around 595 nm. After resting in the dark for 24 h, no modifications in either absorption or emission properties were observed. Spectral similarities of photoconverted chromophores and the blue

chromophore band at 405-408 nm observed at early stages of DsRed1 maturation [28] suggests they are structurally close. Although at present blue-photoconversion would not be suitable for cell biological applications, it could be used in biotechnological approaches to label DsRed-containing immobilized structures by spectrally resolved blue fluorescence.

Some *Anthozoa* CPs *in vitro*, as well as in prokaryotic and eukaryotic cells, exhibit the phenomenon of light-induced emission kindling [11]. It was reported that fluorescence of asulCP was virtually imperceptible at the start of observations but the intensity of the red emission with a peak at 595 nm increased dramatically following 10-20 sec exposure, even to low-intensity green light in the 510-590 nm range. This was reversible since fluorescence decreased to basal levels upon removal of the green illumination. Surprisingly, asulCP red fluorescence could be quenched by blue light at 440-500 nm. This kindling effect strongly depended on irradiation intensity, with brighter light or longer exposure resulting in faster and more pronounced increases and quenching of fluorescence.

Intensive mutagenesis of asulCP produced kindling FP mutants (KFPs) that differed in the duration of their light-induced reversible fluorescent state. Moreover, the asulCP/A148G mutant, when illuminated by high intensity green light, remained kindled irreversibly, and did not undergo quenching upon blue irradiation [117]. AsulCP/A148G was tagged to mitochondria of PC12 cells, and some mitochondria were selectively kindled to study their intracellular dynamics (Fig. 13). This KFP was also successfully used for *in vivo* labeling to monitor *Xenopus* embryo neural plate development by micro-injecting its mRNA into egg poles before cleavage [117]. Recently, an *Aequorea* GFP kindling mutant was also reported [118]. When fused to galactosyltransferase it allowed study of Golgi complex breakdown and reassembly upon photoactivating the Golgi pool of these molecules.

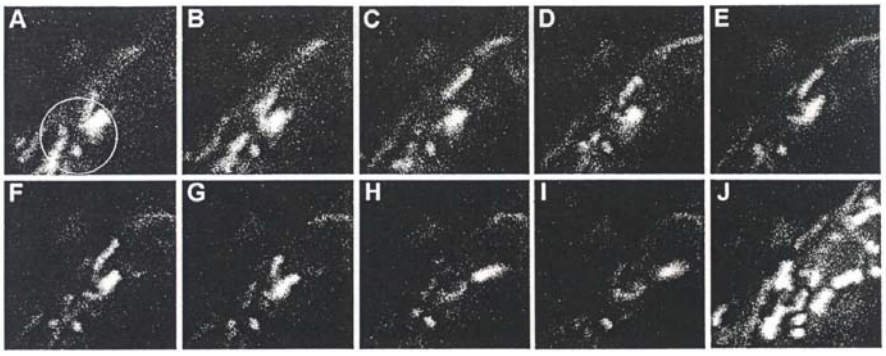

Figure 13. Mitochondria tracking within eukaryotic cell. PC-12 cells expressing asulCP/A148G with a mitochondrial localization signal were examined 48 h after transfection using confocal microscopy (LSM 510, Zeiss, NJ). (A) Mitochondria within the small region (circle) were briefly irradiated (fast mode, 20 sec) by HeNe laser green line (543 nm, 0.3 mW power) causing the asulCP/A148G-containing mitochondria to be irreversibly kindled. (B-I) Irreversibly kindled mitochondria were tracked using 0.05 mW of the same line as the excitation source. Pictures were taken every 10 seconds. (J) A larger part of the cell was briefly irradiated by 1 mW of the laser, causing kindling of the asulCP/A148G in all mitochondria within the visible field.

Use of KFPs to study movement of cells, organelles and tagged proteins has obvious advantages compared to conventional FRAP. It is technically easier and more informative to monitor photo-induced KFP fluorescence than the absence of signal, as with standard FPs upon photobleaching. In the course of experiment, one could also selectively kindle any area of a cell to visualize the spatio-temporal pattern of all KFP-tagged intracellular objects, and subsequently quench them while continuing to monitor irreversibly kindled KFPs. Besides wide biological applications, KFPs can be also used in photoluminescent thin films, photochemical memories and nano-biotechnology, where they may represent attractive alternatives to photoconvertable dyes, energy-transfer fluorospheres and nanocrystal quantum dots [119].

11. Future studies

Four years of progress in studies on the novel family of *Anthozoa* GFP-like proteins has seen their advantages repeatedly enhanced, and disadvantages successfully overcome. Problems due to slow maturation were overcome by the development of fast maturation mutants, nonspecific aggregation was prevented by developing non-aggregating mutants, aggregation of fusion proteins was reduced by monomeric mutants, FP-tandem and "filling by tag" approaches, and secondary green fluorescence was avoided by the development of mutants directed towards the red pathway of chromophore formation. One may ask, what shall we next do with this amazing and expanding palette of GFP-like proteins with an almost rainbow spectrum range? We believe enormous challenges and opportunities are still ahead. It is crucial to resolve more three-dimensional structures of *Anthozoa* FPs that will provide bases for understanding mechanisms, diversity and evolutionary regulation of chromophore formation and oligomerization of these proteins. Because fluorescence of live corals is probably restricted to already cloned *Anthozoa* FPs [22], discovery of naturally occurred CPs with far-red absorption spectra is desirable. Structural studies together with availability of new CPs could prompt residue substitutions, creating fluorescent mutants with shifted emission spectra further into far-red and infra-red regions (650-900 nm), where animal tissues have highest transparency, and creating new photoconvertable mutants and active intracellular biosensors. New generation of laser scanning microscopes that split emission onto multi-channel detectors will overcome the limits of existing multicolor labeling and FRET detection methods. Due to spectral distribution of fluorescence signals as a parameter of every pixel, they allow detection of even tiny spectral changes in FPs, despite spectral overlaps. We also anticipate future use of *Anthozoa* FPs in intact tissues and whole organisms where methods of cDNA introduction, such as "gene gun" and homologous recombination, are well established. The combination of spatio-restricted and deeper multi-photon laser excitation with high-output fiber endoscopy will permit *in situ* FP-based analysis of numerous biological processes in transgenic animals.

Acknowledgements

We thank M.Yanagisawa and S.A.Lukyanov for encouragement and support. This work was supported in part by grants from National Institutes of Health (V.V., M.M.), Russian Academy of Sciences for the program "Physicochemical Biology" (K.L.) and INTAS 2001-2347.

References

1. Wouters, F.S., Verveer, P.J., and Bastiaens, P.I. 2001, Trends Cell Biol., 11, 203-211.
2. Prasher, D.C., Eckenrode, V.K., Ward, W.W., Prendergast, F.G., and Cormier, M.J. 1992, Gene 111, 229-233.
3. Heim, R., Praser, D.C., and Tsien, R.Y. 1994, Proc. Natl. Acad. Sci. USA, 91, 12501-12504.
4. Delagrave, S., Hawtin, R.E., Silva, C.M., Yang, M.M., and Youvan, D.C. Biotechnology (N.Y.), 1995, 13, 151-154.
5. Heim, R., and Tsien, R.Y. 1996, Curr. Biol., 6, 178-182.
6. Ormo, M., Cubitt, A.B., Kallio, K., Gross, L.A., Tsien, R.Y., and Remington, S.J. 1996, Science, 273, 1392-1395.
7. Matz, M.V., Fradkov, A.F., Labas, Y.A., Savitsky, A.P., Zaraisky, A.G., Markelov, M.L., and Lukyanov, S.A. 1999, Nat. Biotechnol., 17, 969-973.
8. Fradkov, A.F., Chen, Y., Ding, L., Barsova, E.V., Matz, M.V., and Lukyanov, S.A. 2000, FEBS Lett., 479, 127-130.
9. Wiedenmann, J., Elke, C., Spindler, K.D., and Funke, W. 2000, Proc. Natl. Acad. Sci. USA, 97, 14091-14096.
10. Labas, Y.A., Gurskaya, N.G., Yanushevich, Y.G., Fradkov, A.F., Lukyanov, K.A., Lukyanov, S.A., and Matz, M.V. 2002, Proc. Natl. Acad. Sci. USA, 99, 4256-4261.
11. Lukyanov, K.A., Fradkov, A.F., Gurskaya, N.G., Matz, M.V., Labas, Y.A., Savitsky, A.P., Markelov, M.L., Zaraisky, A.G., Zhao, X., Fang, Y., Tan, W., and Lukyanov, S.A. 2000, J. Biol. Chem., 275, 25879-25882.
12. Gurskaya, N.G., Fradkov, A.F., Terskikh, A., Matz, M.V., Labas, Y.A., Martynov, V.I., Yanushevich, Y.G., Lukyanov, K.A., and Lukyanov, S.A. 2001, FEBS Lett., 507, 16-20.
13. Wilson. T., and Hastings, J.W. 1998, Annu. Rev. Cell Dev. Biol., 14, 197-230.
14. Chalfie. M., Tu, Y., Euskirchen, G., Ward, W.W., and Prasher, D.C. 1994, Science, 263, 802-805.
15. Cubitt, A.B., Heim, R., Adams, S.R., Boyd, A.E., Gross, L.A., and Tsien, R.Y. 1995, Trends Biochem. Sci., 20, 448-455.
16. Fukuda, H., Arai, M., and Kuwajima, K. 2000, Biochemistry, 39, 12025-12032.
17. Zacharias, D.A., Baird, G.S., and Tsien, R.Y. 2000, Curr. Opin. Neurobiol., 10, 416-421.
18. Tsien, R.Y. 1998, Annu. Rev. Biochem., 1998, 67, 509-544.
19. Johnson, F.H., Shimomura, O., Saiga, Y., Gershman, L.C., Reyholds, G.T., and Waters, J.R. 1962, J. Cell. Comp. Physiol. 60, 85-104.
20. Ward, W. W., and Cormier, M. J. 1979, J. Biol. Chem., 254, 781-788.
21. Dove, S. G., Hoegh-Guldberg, O., and Ranganathan, S. 2001, Coral Reefs, 19, 197-204.
22. Salih, A., Larkum, A., Cox, G., Kuhl, M., and Hoegh-Guldberg, O. 2000, Nature, 408, 850-853.
23. Shimomura, O. 1979, FEBS Lett., 104, 220-222.
24. Cody, C.W., Prasher, D.C., Wastler, W.M., Prendergast, F.G., and Ward, W.W. 1993, Biochemistry, 32, 1212-1218.
25. Yang, F., Moss, L.G., and Phillips, G.N., Jr. 1996, Nat. Biotechnol., 14, 1246-1251.
26. Yarbrough, D., Wachter, R.M., Kallio, K., Matz, M.V., and Remington, S.J. 2001, Proc. Natl. Acad. Sci. USA, 98, 462-467.
27. Baird, G.S., Zacharias, D.A., and Tsien, R.Y. 2000, Proc. Natl. Acad. Sci. USA, 97, 11984-11989.
28. Wiehler, J., von Hummel, J., and Steipe, B. 2001, FEBS Lett., 487, 384-389.
29. Mizuno, H., Sawano, A., Eli, P., Hama, H., and Miyawaki, A. 2001, Biochemistry, 40, 2502-2510.
30. Terskikh, A., Fradkov, A., Ermakova, G., Zaraisky, A., Tan, P., Kajava, A.V., Zhao, X., Lukyanov, S., Matz, M., Kim, S., Weissman, I., and Seibert, P. 2000, Science, 290, 1585-1588.

31. Terskikh, A.V., Fradkov, A.F., Zaraisky, A.G., Kajava, A.V., and Angres B. 2002, J. Biol. Chem., 277, 7633-7636.
32. Gurskaya, N. G., Savitsky, A. P., Yanushevich, Y. G., Lukyanov, S. A., and Lukyanov, K. A. 2001, BMC Biochem., 2, 6.
33. Bulina, M.E., Chudakov, D.M., Mudrik, N.N., and Lukyanov, K.A. 2002, BMC Biochem., 3, 7.
34. Campbell, R.E., Tour, O., Palmer, A.E., Steibach, P.A., Baird, G.S., Zachrias, D.A., and Tsien, R.Y. 2002, Proc. Natl. Acad. Sci. USA, 99, 7877-7882.
35. Remington, S.J. 2000, Meth. Enzymol., 305, 196-211.
36. Gross, L.A., Baird, G.S., Hoffman, R.C., Baldridge, K.K., and Tsien, R.Y. 2000, Proc. Natl. Acad. Sci. USA, 97, 11990-11995.
37. Wall, M.A., Socolich, M., and Ranganathan, R. 2000, Nat. Struct. Biol., 7, 1133-1138.
38. He, X., Bell, A.F., Tonge, P.J. 2002, Org. Lett., 4, 1523-1526.
39. Kupfer R., Meler S., and Wurthwein E.U. 1984, Synthesis, 1984, 688-690.
40. Malassa I., and Matthies D. 1987, Chemiker-Zeitung, 111, 253-261.
41. Remington, S.J. 2002, Nat. Biotechn., 20, 28-29.
42. Martynov, V.I., Savitsky, A.P., Martynova, N.Y., Savitsky, P.A., Lukyanov, K.A., Lukyanov, S.A.. 2001, J. Biol. Chem., 276, 21012-21016.
43. Savitsky, A. P., Lukyanov, K. A., Gurskaya, N. G., Savitsky, P. A., Matz, M. V., Fradkov, A. F., and Lukyanov, S. A. 2000, 11-th International Symposium on Bioluminescence and Chemoluminescence, Sept. 6-10, Pacific Grove, CA.
44. Vrzheshch, P.V., Akovbian, N.A., Varfolomeyev, S.D. and Verkhusha, V.V. 2000, FEBS Lett., 487, 203-208.
45. Verkhusha, V.V., Akovbian, N.A., Efremenko, E.N., Varfolomeyev S.D., and Vrzheshch, P.V. 2001, Biochemistry (Mosc.), 66, 1342-1351.
46. Yanushevich, Y.G., Staroverov, D.b., Savitsky, A.P., Fradkov, A.F., Gurskaya, N.G., Bulina, M.E., Lukyanov, K.A., and Lukyanov, S.A. 2002, FEBS Lett., 511, 11-14.
47. Heikai, A.A., Hess, S.T., Baird, S.G., Tsien, R.Y., and Webb, W.W. 2000, Proc. Natl. Acad. Sci. USA, 97, 11996-12001.
48. Culter, M.W., and Ward, W.W. 1997, in Bioluminescence and Chemiluminescence: Molecular Reporting with Photons, J.W. Hastings, L.J. Kriska, and P.E. Stanley (Eds.), Wiley & Sons, New York, 403-406.
49. Verkhusha, V.V., Otsuna, H., Awasaki, T., Oda, H., Tsukita, S., and Ito, K. 2001, J. Biol. Chem., 276, 29621-29624.
50. Ward, W.W. 1998, in Green Fluorescent Protein: Properties, Applications, and Protocols, M.Chalfie, and S.Kain (Eds.), Wiley-Liss, New York, 45-75.
51. Niwa, H., Inouye, S., Hirano, T., Matsuno, T., Kojima, S., Kubota, M., Ohashi, M., and Tsuji, F.I. 1996, Proc. Natl. Acad. Sci. USA, 93, 13617-13622.
52. Weber, W., Helms, V., McCammon, J.A., and Langhoff, P.W. 1999, Proc. Natl. Acad. Sci. USA 96, 6177-6182.
53. Bevis, B.J., and Glick, B.S. 2002, Nat. Biotechnol., 20, 83-87.
54. Harms, G.S., Cognet, L., Lommerse, P.H., Blab, G.A., and Schmidt, T. 2001, Biophys. J., 80, 2396-2408.
55. Pepperkok, R., Squire, A., Geley, S., and Bastiaens, P.I. 1999, Curr. Biol., 9, 269-272.
56. Jakobs, S., Subramaniam, V., Schonle, A., Jovin, T.M., and Hell, S.W. 2000, FEBS Lett., 479, 131-135.
57. Cotlet, M., Hofkens, J., Habuchi, S., Dirix, G., van Guyse, M., Michiels, J., Vanderleyden, J., and de Schryver, F.C. 2001, Proc. Natl. Acad. Sci. USA, 98, 14398-14403.
58. Malvezzi-Campeggi, F., Jahnz, M, Heinze, K.G., Dittrich, P., and Schwille, P. 2001, Biophys. J., 81, 1776-1785.
59. Schottrigkeit, T.A., Zachariae, U., von Fellitzsch, T., Wiehler, J., von Hummel, J., Steipe, B., and Michel-Beyerle, M.E. 2001, ChemPhysChem, 2, 325-328.

60. Garcia-Parajo, M.F., Koopman, M., van Dijk, E.M., Subramaniam, V., and van Hulst, N.F. 2001, Proc. Natl. Acad. Sci. USA, 98, 14392-14397.
61. Lounis, B., Deich, J., Rosell, F.I., Boxer, S.G., and Moerner, W.E. 2001, J. Phys. Chem. B, 105, 5048-5054.
62. Cotlet, M., Hofkens, J., Kohn, F., Michiels, J., Diris, G., van Guyse, M., Vanderleyden, J., and de Schryver, F.C. 2001, Chem. Phys. Lett., 336, 415-423.
63. Visser, N.V., Hink, M.A., Borst, J.-W., van der Krogt, G.N., and Visser, A.J. 2002, FEBS Lett., 521, 31-35.
64. Bulina, M.E., Verkhusha, V.V., Staroverov, D.B., Chudakov, D.M., and Lukyanov, K.A. 2003, Biochem. J., 371, 109-114.
65. Reid, B. G., and Flynn, G. C. 1997, Biochemistry, 36, 6786-6791.
66. Verkhusha, V.V., Kuznetsova, I.M., Stepanenko, O.V., Zaraisky, A.G., Shavlovsky, M.M., Turoverov, K.K., and Uversky, V.N. 2003, Biochemistry, 42, 7879-7884.
67. Catala, R. 1959, Nature, 183, 949.
68. Kawaguti, S. 1944, Palao Trop. Biol. Stn. Stud., 2, 617-674.
69. Schlichter, D., and Fricke, H. W. 1990, Naturwissenschaften, 77, 447-450.
70. Mazel, C. H. 1995, Marine Ecology-Progress Series, 120, 185-191.
71. Mazel, C. H. 1997, Ocean Optics XIII, Proc. SPIE, 2963, 240-245.
72. Veron, J. E. N. 2000, in Corals of the World. Austr. Inst. Mar. Sci., Townsville, MC.
73. Fox, D. L. 1974, in The Significance of Zoochromes, A. E. Needham (Ed.), Springer Verlag, New York.
74. Wicksten, M. K. 1989, Bull. Mar. Sci., 45, 519-530.
75. Mobley, C. D., 1994, in Radiative Transfer in Natural Waters. Academic Press.
76. Kuhl, M., Cohen, Y., Dalsgaard, T., Jorgensen, B. B., and Revsbech, N. P. 1995, Marine Ecology-Progress Series, 117, 159-172.
77. Maksimow, M., Hakkila, K., Karp, M., and Vitra, M. Cytometry, 2002, 47, 243-247.
78. Rodrigues, F., van Hemert, M., Steensma, H.Y., Corte-Real, M., and Leao, C. 2001, J. Bacteriol., 183, 3791-3794.
79. Jach, G., Binot, E., Frings, S., Luxa, K., and Schell, J. 2001, Plant J., 26, 483-491.
80. Dietrich, C., and Maiss, E. 2001, Biotechniques, 32, 286-293.
81. Handler, A.M., and Harrell, R.A. Biotechniques, 2001, 31, 820-828.
82. Nolan, T., Bower, T.M., Brown, A.E., Crisanti, A., and Catteruccia, F. 2002, J. Biol. Chem., 277, 8759-8762.
83. Werdien, D., Peiler, G., and Ryffel, G.U. 2001, Nucleic Acid Res., 29, E53.
84. Finley, K.R., Davidson, A.E., and Ekker, S.C. 2001, Biotechniques, 31, 66-72.
85. Hawley, T.S., Telford, W.G., Ramezani, A., and Hawley, R.G. 2001, Biotechniques, 30, 1028-1034.
86. Moede, T., Leibiger, B., Berggren, P.O., Leibiger, I.B. 2001, Diabetes, 50, S15-S19.
87. Yang, Y.S., and Hughes, T.E. 2001, Biotechniques, 31, 1036-1041.
88. Hakkila, K., Maksimow, M., Karp, M., and Vitra, M. Anal. Biochem., 2002, 301, 235-242.
89. Engqvist-Goldstein, A.E., Warren, R.A., Kesseles, M.M., Keen, J.H., Heuser, J., and Drubin, D.G. 2001, J. Cell Biol., 154, 1209-1223.
90. Nelson, G., Paraoan, L., Spiller, D.G., Wilde, G.J., Browne, M.A., Djali, P.K., Unitt, J.F., Sullivan, E., Floettmann, E., and White, M.R. 2002, 115, 1137-1148.
91. Charpilienne, A., Nejmeddine, M., Berois, M., Parez, N., Neumann, E., Hewat, E., Trugnan, G., and Cohen, J. 2001, J. Biol. Chem., 276, 29361-29367.
92. Bloemberg, G.V., Wijfjes, A.H., Lamers, G.E., Stuurman, N., and Lugtenberg, B.J. 2000, Mol. Plant Microbe Interact., 13, 1170-1176.
93. Peloquin, J.J., Lauzon, C.R., Potter, S., and Miller, T.A. 2002, Curr. Microbiol., 45, 41-45.
94. Maselli, A., Laevsky, G., and Knecht, D.A. 2002, Microbiology, 148, 413-420.

95. Datwyler, D.A., Magyar, J.P., Busceti, V., Hirschy, A., Perriard, J.C., Bailey, J.E., and Eppenberger, H.M. 2001, Basic Res. Cardiol., 96, 630-635.
96. Furuta, T., Tomioka, R., Taki, K., Nakamura, K., Tamamaki, N., and Kaneko, T. 2001, J. Histochem. Cytochem., 49, 1497-1508.
97. Lauf, U., Lopez, P., and Falk, M.M. 2001, FEBS Lett., 498, 11-15.
98. Fradkov, A.F., Verkhusha, V.V., Staroverov, D.B., Bulina, M.E., Yanushevich, Y.G., Martynov, V.I., Lukyanov, S., and Lukyanov, K.A. 2002, Biochem. J., 368, 17-21.
99. Qin, H., Shao, Q., Belliveau, D.J., and Laird, D.W. 2001, Cell Adhes. Commun., 8, 433-439.
100. Forster, V.T. 1948, Ann. Phys., 6, 54-75.
101. Pollok, B.A., and Heim, R. 1999, Trends Cell Biol., 9, 57-60.
102. Selvin, P.R. 2000, Nat. Struct. Biol., 7, 730-734.
103. Patterson, G.H., Piston, D.W., and Barisas, B.G. 2000, Anal. Biochem., 284, 438-440.
104. Miyawaki, A., and Tsien, R.Y. 2000, Methods Enzymol., 327, 472-500.
105. Miyawaki, A., Llopis, J., Heim, R., McCaffery, J.M., Adams, J.A., Ikura, M., and Tsien, R.Y. 1997, Nature, 388, 882-887.
106. Mas, P., Devlin, P.F., Panda, S., and Kay, S.A. 2000, Nature, 408, 207-211.
107. Mitra, R.D., Silva, C.M. and Youvan, D.C. 1996, Gene, 173, 13-17.
108. Zlokarnik, G., Negulescu, P.A., Knapp, T.E., Mere, L., Burres, N., Feng, L., Whitney, M., Roemer, K., and Tsien, RY. 1998, Science, 279, 84-88.
109. Griffin, B.A., Adams, S.R., and Tsien, R.Y. 1998, Science, 281, 269-272.
110. Xu, Y., Piston, D.W., and Johnson, C.H. 1999, Proc. Natl. Acad. Sci. USA, 96, 151-156.
111. Angers, S., Salahpour, A., Joly, E., Hilairet, S., Chelsky, D., Dennis, M., and Bouvier, M. 2000, Proc. Natl. Acad. Sci. USA, 97, 3684-3689.
112. Li, M., and Selvin, P.R. 1995, J. Am.Chem. Soc., 117, 8132-8138.
113. Cha, A., Snyder, G.E., Selvin, P.R., and Bezanilla, F. 1999, Nature, 402, 809-813.
114. Bader, B., Butt, E., Palmetshofer, A., Walter, U., Jarchau, T., and Drueckes, P. 2001, J. Biomol. Screen., 6, 255-264.
115. Lippincott-Schwartz, J., Snapp, E., and Kenworthy, A. 2001, Nat. Rev. Mol. Cell Biol., 2, 444-455.
116. Marchant, J.S., Stutzmann, G.E., Leissring, M.A., LaFerla, F.M., and Parker, I. 2001, Nat. Biotechnol., 19, 645-649.
117. Chudakov, D.M., Belousov, V.V., Zaraisky, A.G., Novoselov, V.V., Staroverov, D.B., Zorov, D.B., Lukyanov, S., and Lukyanov, K.A. 2003, Nat. Biotechnol. 21, 191-194.
118. Patterson, G.H., and Lippincott-Schwartz, J. 2002, Science, 297, 1873-1877.
119. Lacoste, T.D., Michalet, X., Pinaud, F., Chemla, D.S., Alivisatos, A.P., and Weiss, S. 2000, Proc. Natl. Acad. Sci. USA, 97, 9461-9466.